Some Aspects of Cosmic Synchrotron Sources

by

Richard I. Epstein

March 1973

SUIPR Report No. 435

Office of Naval Research
Contract N00014-67-A-0112-0062
National Aeronautics and Space Administration
Grant NGL 05-020-272
National Science Foundation
Grant GP-23840

INSTITUTE FOR PLASMA RESEARCH
STANFORD UNIVERSITY, STANFORD, CALIFORNIA

SOME ASPECTS OF COSMIC SYNCHROTRON SOURCES

by

Richard I. Epstein*

Office of Naval Research
Contract N00014-67-A-0112-0062

National Aeronautics and Space Administration
Grant NGL 05-020-272

National Science Foundation
Grant GP-23840

SUIPR Report No. 435

March 1973

Institute for Plasma Research
Stanford University
Stanford, California

*Present address: University of Texas at Austin
Astronomy Department
Austin, Texas

DEDICATED TO

MY PARENTS

JACOB AND BEATRICE

ABSTRACT

In the earlier treatments of synchrotron theory it was usually assumed that the pitch angles of the radiating particles are of the order of unity and that the emission occurs at high harmonics of the fundamental frequency. In this investigation we have examined synchrotron radiation for some of the cases for which these assumptions are not applicable. We first considered the synchrotron emission from individual particles which have small pitch angles, the general properties of synchrotron sources which mainly contain such particles, and the emissivities and degrees of circular polarization for specific source distributions. We then considered several models for actual synchrotron sources. The limitation of synchrotron source models for optical pulsars and compact extragalactic objects are discussed and it is shown that several existing models for the pulsar NP 0532 are inconsistent with the measured time variations and polarizations of the optical emission. We also consider whether the low frequency falloffs in the extragalactic objects PKS 2134 + 004, OQ 208 and NGC 1068 could be due to emission from particles with small pitch angles or absorption by a thermal plasma or synchrotron self-absorption. Emission by particles with small pitch angles could explain the observations of PKS 2134 + 004 and OQ 208 but is inconsistent with the data for NGC 1068. The absorption interpretations cannot account for the turnover in the spectrum of PKS 2134 + 004. Measurements of polarization, angular structure and x-ray flux which would be helpful in evaluating these models are described.

ACKNOWLEDGMENT

This investigation was carried out under the direction of Peter Sturrock whose suggestions and encouragement have stimulated much of this work, especially Sections 2II and 3II. It has also been a pleasure to work with Vahé Petrosian; we collaborated on the material in Chapter 3, and he has made useful criticisms concerning the other parts of this study. Bill Adams, Spiro Antiochos, Chuck Newman, Dave Roberts, Chris McKee, Reuven Ramaty and Ronald Bracewell have read at least portions of the various drafts of the manuscript and have made a number of important comments. Gary McDonough has been a friend and reliable counselor through much of my graduate school career, and B Fahr was an indispensible compatriot in the preparation of the first complete version of this work. I am grateful to Evelyn Mitchell for her very competent help in arranging and typing this report.

This work has been supported by the National Aeronautics and Space Administration under Grant NGL 05-020-272, the National Science Foundation under Grant GP-23840 and the Office of Naval Research under Contract N00014-67-A-0112-0062.

TABLE OF CONTENTS

LIST OF TABLES

LIST OF ILLUSTRATIONS

Chapter 1

INTRODUCTION

Synchrotron radiation (or the more descriptive terms magneto-bremsstrahlung and magnetic bremsstrahlung) refers to the emission from a highly relativistic charged particle which is accelerated by a magnetic field. Much of the theory of this process has been known for at least sixty years, although no recognized observations of this type of emission were made until the late 1940's when intense visible radiation was observed from the relativistic electrons circling in the General Electric synchrotron (Elder, Langmuir and Pollock, 1948). Shortly after these first laboratory observations, Alfvén and Herlofson (1950) suggested that the emission from "radio stars" might also be due to the synchrotron process, and later Shklovsky proposed that part of the optical emission from the Crab nebula could be produced by this mechanism. Since it was known that synchrotron radiation is for the most part linearly polarized, the subsequent detection of linear polarization in the optical radiation from the Crab nebula (Oort and Walraven, 1956) and the jet of M87 (Baade, 1956), and in the general galactic radio emission (Razin, 1958) gave strong support to these early theories. It is now generally believed that synchrotron radiation is responsible for at least part of the continuous spectra from many cosmic phenomena, for instance radio galaxies, quasars, supernova remnants, galactic radio emission, the Jovian bursts and solar flares.

Much of the current work on cosmic synchrotron emission is directed toward deciding which sources are emitting synchrotron radiation and analyzing the emission to determine their physical nature. In order

to deal with these questions one needs to be familiar with the various aspects of the synchrotron mechanism and related processes, for instance (1) the emission spectra and polarization for possible particle ensembles which might exist in astronomical objects, (2) the effects of an ambient thermal gas on synchrotron emission and the propagation of radiation, and (3) the additional emission processes which may occur in conjunction with synchrotron emission, such as the inverse Compton effect (the production of high frequency radiation due to the scattering of low frequency radiation by relativistic particles).

Some important analyses and good reviews of these topics can be found in the following articles: Schwinger (1949; spectrum and angular distribution); Westfold (1959; linear polarization); LeRoux (1961; linear polarization); Ginzburg and Syrovatskii (1965 and 1969; reviews which include effects of self-absorption and of an ambient plasma); Blumenthal and Gould (1970; review of radiation processes); Pacholczyk (1970; review of radio astrophysics). The work prior to 1968 contained some errors concerning radiation from particles in non-circular orbits (Epstein and Feldman, 1967), but this has been amended in the more recent publications.

In most of the existing applications of synchrotron theory to astrophysics it has been assumed that the relativistic electrons are oriented isotropically, or nearly so. This is almost certainly a good approximation for extended sources (the large double or halo structures in radio galaxies, the remnants of supernova, and the general galactic radio emission) where interaction with the ambient medium would destroy any large anisotropies in the velocity distributions of the cosmic rays.

For more compact sources (such as quasars, active galactic nuclei, and pulsars), however, the pressure of the relativistic particles may be great enough to induce streaming along the magnetic fields. It has been suggested that at least part of the emission from quasars and active galaxies (Woltjer, 1966; Noerdlinger, 1969; Cavaliere et al., 1970) and from pulsars (Shklovsky, 1970; Sturrock, 1971; Zheleznyakov, 1971) is synchrotron radiation from electrons which have small pitch angles (the pitch angle, Ψ, is the constant angle between the velocity of the particle and the magnetic field).

In this present investigation, we extend the existing analyses of synchrotron theory to include the radiation from particles with small pitch angles and apply these results to several problems in astrophysics. Chapter 2 contains the theoretical developments: (1) the analysis of the emission from individual particles, (2) a general treatment of synchrotron emission from cosmic sources and (3) the computation of the emissivity for three illustrative source distributions. In Chapter 3 we examine a number of models for the emission from astronomical objects. (1) Some restrictions are placed on the allowable models of the optical emission from NP 0532. (2) Several theoretical models for the low frequency cutoffs in the radio emission from PKS 2134 + 004 (a quasar) and OQ 208 (a Seyfert galaxy) and in the infrared emission from NGC 1068 (a Seyfert galaxy) are discussed and compared. Some of these proposed models are ruled out and observational tests for the other models are suggested.

Chapter 2

EXTENSION OF SYNCHROTRON THEORY FOR SMALL PITCH ANGLES

I. Introduction

The conventional analyses of synchrotron theory, in which it is assumed that the pitch angle, Ψ, between the particle velocity and the magnetic field is of the order of unity, are adequate for the discussion of many astrophysical phenomena; however, some of the observable radiation from quasars, galactic nuclei and pulsars may be emitted by particles which have small pitch angles. Several authors (O'Dell and Sartori, 1970b; Cavaliere et al., 1970) have suggested that in some sources the radiating particles may even satisfy the more stringent condition $\Psi \leqslant \gamma^{-1} \equiv mc^2/E$ (where E is the energy of the particle). This present investigation deals with the special features of synchrotron radiation which occur when the radiating particles have small pitch angles. Other workers have dealt with aspects of this problem (O'Dell and Sartori, 1970a,b; Melrose, 1971a; Tademaru, 1972), and their contributions are also discussed.

In Section II the emission from individual particles is examined. First, we obtain expressions for the emission from a particle which has a very small pitch angle $\Psi \ll \gamma^{-1}$, and then we consider the more general case in which the restriction on the pitch angle of the particle is only $\Psi \ll 1$; exact and approximate expressions are presented. In Section III we derive expressions for the emissivity, degree of circular polarization and maximum degree of linear polarization for optically thin synchrotron sources in which the particles mainly have small pitch angles and stream along somewhat irregular magnetic fields. The emission

for several source distributions is computed in Section IV, and the main results of the chapter are summarized in Section V.

II. Synchrotron Radiation from Individual Particles

A) Radiation from Particles with Very Small Pitch Angles

While the general analysis of synchrotron radiation from a particle which spirals in a magnetic field is fairly involved, we can gain some understanding of synchrotron radiation from particles with small pitch angles and derive some useful formulas by first limiting the discussion to particles with very small pitch angles.

For the special case of a single, isolated (in a vacuum), highly relativistic particle ($\gamma \gg 1$) which has a very small pitch angle ($\Psi \ll \gamma^{-1}$), the problem of computing the synchrotron emission is greatly simplified. Designate the inertial frame of the observer by K and call the inertial frame in which the particle orbit is circular the K_o frame. K_o moves relative to K with a velocity $c\underset{\sim}{\beta}_{\|}$ where $\beta_{\|}$ is the magnitude of the particle velocity along the magnetic field, $\beta_{\|} = |\underset{\sim}{\beta}_{\|}| = \beta \cos\Psi$, and $\beta = \sqrt{1-\gamma^{-2}}$. As seen in K_o, the normalized velocity of the particle is

$$\beta_o = \frac{\sqrt{\gamma^2-1}\,\sin\Psi}{\sqrt{\cos^2\Psi + \gamma^2\sin^2\Psi}} \approx \gamma\Psi \ll 1 \qquad (2.1)$$

(quantities which are measured in K_o are subscripted with o). When $\gamma\Psi \ll 1$, the particle energy in K_o is non-relativistic so that to observers in this frame the emission appears to be mainly monochromatic cyclotron radiation. The particle emissivity in K_o can be written as (Bekefi, 1966)

$$\eta_o = \frac{\pi e^2 \beta_o{}^2 \nu_B{}^2}{2c} (1 + \cos^2\theta_o)\, \delta(\nu_o - \nu_B) \quad \text{erg(sec str Hz)}^{-1} \qquad (2.2)$$

The angle between the direction of emission $\underset{\sim}{k}_o$ and $\underset{\sim}{B}$ is given by θ_o; $\nu_B = |eB/2\pi mc|$; e is the charge of the particle; and $B = |\underset{\sim}{B}|$.

The radiation is completely polarized and the major axis of the polarization ellipse is in the $\underset{\sim}{k}_o \times \underset{\sim}{B}$ direction. The degrees of linear and circular polarization are*

$$\rho_{\ell o} = \frac{1 - \cos^2\theta_o}{1 + \cos^2\theta_o}$$

$$\rho_{co} = \mu \frac{2 \cos \theta_o}{1 + \cos^2\theta_o} \qquad (2.3)$$

where $\mu = \text{sign}(-e \underset{\sim}{\beta}_{\parallel} \cdot \underset{\sim}{B})$. $\rho_{co} > 0$ for right-hand elliptically polarized radiation (the electric vector moves counter-clockwise as seen by the observer). The quantities $F_o \equiv \int \eta_o d\nu_o$, $F_{\ell o} \equiv \int \rho_{\ell o} \eta_o d\nu_o$ and $F_{co} \equiv \int \rho_{co} \eta_o d\nu_o$ are shown in Figure 1. The degrees of linear and circular polarization are $F_{\ell o}/F_o$ and F_{co}/F_o, respectively. While the emission is, in general, elliptically polarized, it is circularly polarized at $\theta_o = 0$ and $\theta_o = \pi$ (with the opposite sense in each hemisphere) and linearly polarized at $\theta_o = \pi/2$.

---

*By "the degree of linear polarization" we mean the apparent degree of linear polarization which would be detected if the emission was analyzed with antennas that were sensitive to only linearly polarized radiation. Similarly, the "degree of circular polarization refers to the relative difference which would be recorded by antennas that were sensitive to only right- or left-hand circularly polarized radiation. In terms of the Stokes parameters (Ginzburg and Syrovatskii, 1965) the degree of linear polarization and the degree of circular polarization are given by $\sqrt{Q^2 + U^2}/I$ and V/I, respectively.

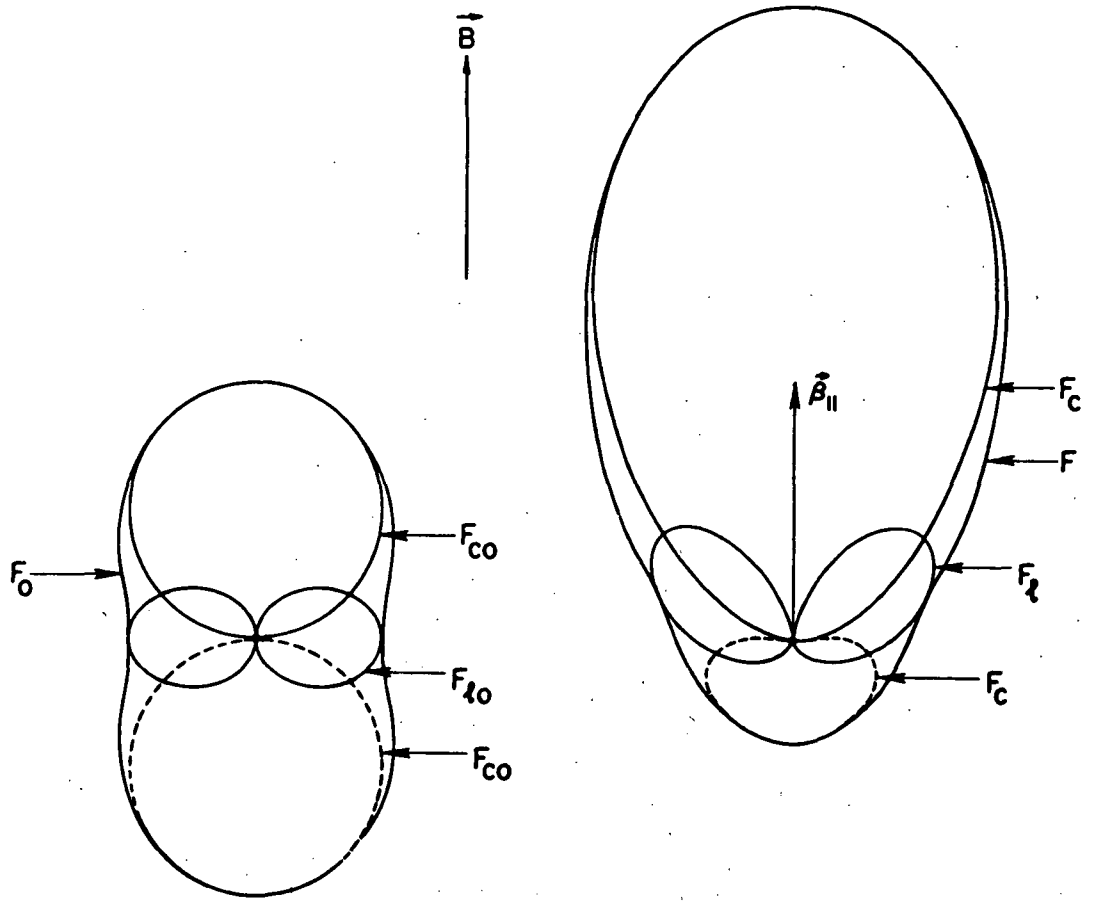

Fig. 1. Angular distribution of the intensity and polarization for the emission from a particle with a very small pitch angle. The figure on the left is the pattern for the non-relativistic cyclotron radiation which would be observed in K_o. The figure on the right is the radiation pattern as seen in the laboratory frame, K, when $\beta_{\parallel} = .3$. The sense of the elliptical polarization is opposite for the solid and dashed F_c curves.

By using the transformations

$$\tan\theta = \frac{\sin\theta_o(1-\beta_{\parallel}^2)^{1/2}}{\cos\theta_o + \beta_{\parallel}} \tag{2.4}$$

$$\nu = \nu_o \frac{(1-\beta_{\parallel}^2)^{1/2}}{1 - \beta_{\parallel}\cos\theta} \tag{2.5}$$

$$\eta = \eta_o \frac{(1 - \beta_\parallel{}^2)^{3/2}}{(1 - \beta_\parallel \cos\theta)^2} \tag{2.6}$$

we can obtain expressions for the radiation as seen in the K frame. It has been assumed here that $\underset{\sim}{\beta}_\parallel$ is parallel to $\underset{\sim}{B}$; when $\underset{\sim}{\beta}_\parallel$ and $\underset{\sim}{B}$ are anti-parallel, θ and θ_o in equations (2.4) through (2.9) should be replaced by $\pi-\theta$ and $\pi-\theta_o$, respectively. The effects of these transformations are illustrated in Figure 1 where $F = \int \eta d\nu$, $F_\ell \equiv \int \rho_\ell \eta d\nu$ and $F_c \equiv \int \rho_c \eta d\nu$ are shown for $\beta_\parallel = .3$. The radiation is beamed and amplified in the direction of $\underset{\sim}{\beta}_\parallel$, and the frequency is Doppler shifted according to equation (2.5): at $\theta = 0$ it is "blue shifted" to $\nu_B\sqrt{(1+\beta_\parallel)/(1-\beta_\parallel)}$, whereas at $\theta = \pi$ it is redshifted to $\nu_B\sqrt{(1-\beta_\parallel)/(1+\beta_\parallel)}$.

The expressions for the emissivity and polarization of the radiation as observed in K are*

$$\eta = \frac{\pi e^2 \gamma \Psi^2 \nu^3}{\nu_B c} \left[1 - \frac{\nu}{\gamma \nu_B} + \frac{\nu^2}{2\gamma^2 \nu_B{}^2}\right] \delta\left(\nu - \frac{2\gamma\nu_B}{1 + \theta^2\gamma^2}\right) \tag{2.7}$$

$$\rho_c = \mu \frac{1 - \theta^4\gamma^4}{1 + \theta^4\gamma^4} = \frac{2\mu\,\gamma\nu_B(\nu - \gamma\nu_B)}{\nu^2 - 2\gamma\nu\nu_B + 2\gamma^2\nu_B{}^2} \tag{2.8}$$

---

*η is the energy emitted by the particle per unit solid angle, time and frequency; however, this is not the observed emissivity. The particle is moving toward the observer in K with a mean velocity $c\beta\cos\theta\cos\Psi$; so that the energy which is emitted in a time dt_e is received in a time $dt_r = dt_e\,(1 - \beta\cos\theta\cos\Psi)$. If the "apparent emissivity" η_a is defined as $\eta_a = \eta/(1 - \beta\cos\theta\cos\Psi)$, then $\eta_a d\Omega$ is the energy received per unit time and frequency by an observer who subtends a solid angle $d\Omega$. To calculate the emission from time independent collections of particles, as is done in Section IV, only the emissivity η has to be used. A good discussion of the distinction between the emissivity and the apparent emissivity is given by Ginzburg and Syrovatskii (1969). In their notation $\eta = r^2 p$ and $\eta_a = r^2\tilde{p}$.

$$\rho_\ell = \frac{2\theta^2\gamma^2}{1 + \theta^4\gamma^4} = \frac{\nu(2\gamma\,\nu_B - \nu)}{\nu^2 - 2\gamma\nu\nu_B + 2\gamma^2\nu_B^2} \quad . \tag{2.9}$$

Only the terms of lowest order in $\psi\gamma$ and θ have been retained.

In any given direction the emission is monochromatic with a frequency $2\gamma\nu_B/(1+\theta^2\gamma^2)$ and elliptically polarized with the major axis of the polarization ellipse aligned with $\underset{\sim}{k} \times \underset{\sim}{B}$. By integrating η over all directions of emission the power spectrum of the total emission from a single particle is found.

$$H(\nu,\gamma,\psi,B) \equiv 2\pi\int \eta \sin\theta \, d\theta \qquad \text{erg(sec Hz)}^{-1}$$

$$= \begin{cases} \dfrac{2\pi^2e^2\psi^2}{c}\,\nu\left[1 - \dfrac{\nu}{\gamma\nu_B} + \dfrac{1}{2}\left(\dfrac{\nu}{\gamma\nu_B}\right)^2\right] & \dfrac{\nu_B}{\gamma} \ll \nu \lesssim 2\gamma\nu_B \\ 0 & \nu > 2\gamma\nu_B \end{cases} \quad . \tag{2.10}$$

The rate of energy loss for the particle is obtained by integrating H over all frequencies

$$-\frac{dE}{dt} = \int_0^\infty H d\nu = \frac{8\pi^2e^2\nu_B^2\gamma^2\psi^2}{3c} \quad . \tag{2.11}$$

Equation (2.11) is in agreement with the general expression for the power radiated by a particle in a magnetic field (Blumenthal and Gould, 1970).

$H(\nu)$, $\rho_\ell(\nu,\theta)$ and $\rho_c(\nu,\theta)$ are shown in Figure 2. The relationship of these expressions to observable quantities is discussed in Section III.

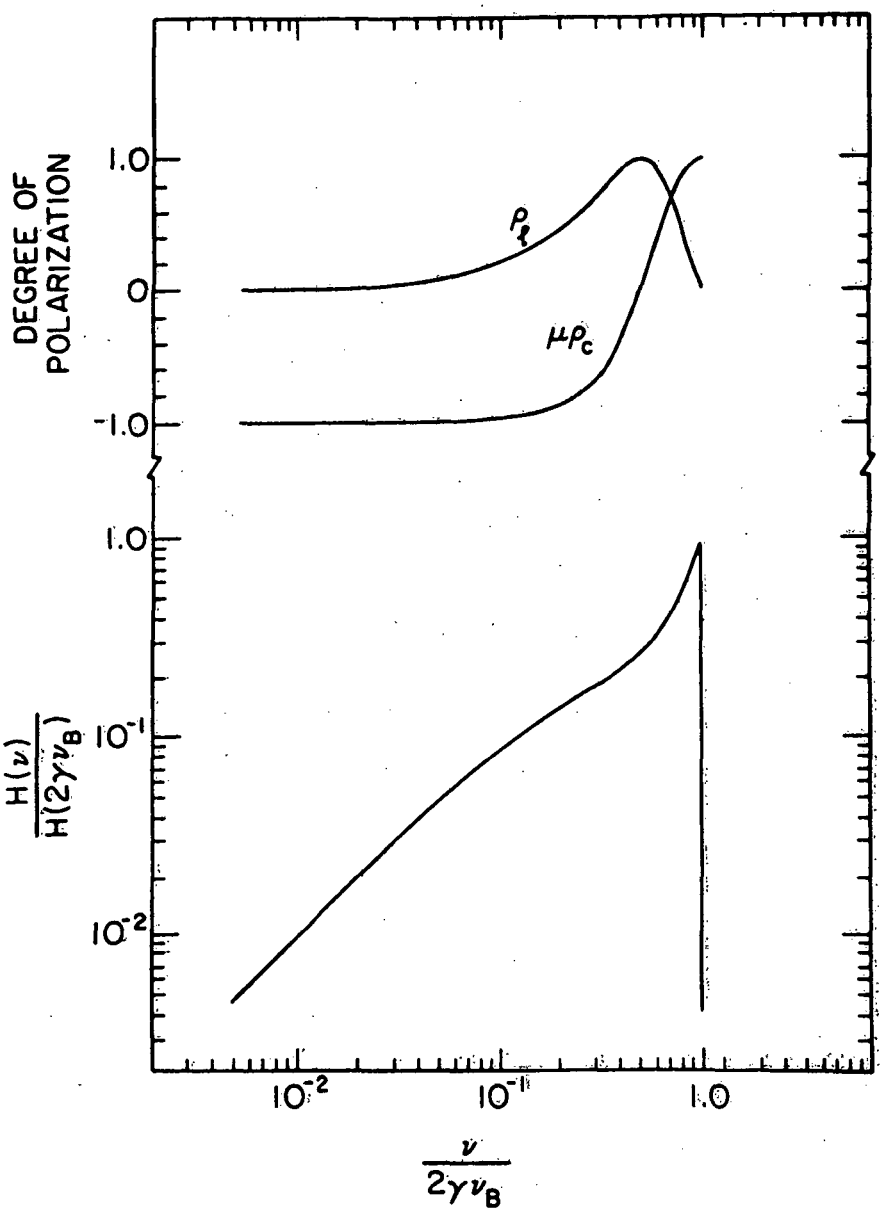

Fig. 2. The emissivity per unit frequency and the polarization of the emission from relativistic particles which spiral with very small pitch angles.

B) Radiation from Particles with Small Pitch Angles

We will now relax the restriction that $\Psi \ll \gamma^{-1}$ and obtain expressions for the particle emissivity with the weaker condition $\Psi \ll 1$. The radiation field of a highly relativistic charged particle

which spirals with arbitrary pitch angle is well known (Ginzburg and Syrovatskii, 1969). If we neglect the effects of any ambient medium, the electric field in the $\underset{\sim}{k}$ direction and at large distance r from the particle can be expressed as

$$\left.\begin{aligned}
\underset{\sim}{\mathcal{E}} &= \mathrm{Re} \sum_{n=1}^{\infty} \underset{\sim}{\mathcal{E}}_n \exp[2\pi\, i\nu_n(r/c) - t)] \\
\underset{\sim}{\mathcal{E}}_n &= \frac{4\pi e \nu_B \sin\Psi}{cr\gamma(1 - \beta\cos\theta\cos\Psi)^2} \left\{ \underset{\sim}{e}_1 J_n'(Z_n) - i\underset{\sim}{e}_2 \frac{(\cos\theta - \beta\cos\Psi)}{\beta\sin\theta\sin\Psi} J_n(Z_n) \right\} \\
Z_n &= \frac{n\beta\sin\theta\sin\Psi}{1 - \beta\cos\theta\cos\Psi} \\
\nu_n &= \frac{n\nu_B}{\gamma(1 - \beta\cos\theta\cos\Psi)}
\end{aligned}\right\} \quad (2.12)$$

The unit vectors $\underset{\sim}{e}_1$ and $\underset{\sim}{e}_2$ are in the $\underset{\sim}{B} \times \underset{\sim}{k}$ and $\underset{\sim}{k} \times (\underset{\sim}{B} \times \underset{\sim}{k})$ directions, respectively; $J_n(x)$ is the Bessel function of order n; and $J_n'(x) = \frac{d}{dx}(J_n(x))$.

The emissivity of the particle is

$$\eta = \frac{r^2 c}{8\pi} (1 - \beta\cos\theta\cos\Psi) \sum_{n=1}^{\infty} |\underset{\sim}{\mathcal{E}}_n|^2 \delta(\nu - \nu_n) \ . \qquad (2.13)$$

The factor $(1 - \beta\cos\theta\cos\Psi)$ adjusts for the average motion of the particle along the magnetic field (see the previous footnote).

Most of the radiation is beamed within an angle of the order of γ^{-1} of the direction of the particle velocity. Since the pitch angle is also small, the emission is mainly confined to limited range of θ: $\theta \leqslant (\Psi + \gamma^{-1}) \ll 1$. By retaining only the terms of the lowest order

in θ, Ψ and γ^{-1} the expression for the emissivity reduces to

$$\left.\begin{aligned} \eta &= \frac{16\pi\, e^2 \nu_B^2 \gamma^4 \Psi^2}{c(1+\theta^2\gamma^2+\Psi^2\gamma^2)} \sum_{n=1}^{\infty} n^2 \left[\left\{J_n'(Z_n)\right\}^2 + \left\{\frac{1-\theta^2\gamma^2+\Psi^2\gamma^2}{2\theta\Psi\gamma^2} J_n(Z_n)\right\}^2\right] \delta(\nu-\nu_n) \\ \nu_n &= \frac{2n\gamma\nu_B}{(1+\theta^2\gamma^2+\Psi^2\gamma^2)} \\ Z_n &= \frac{2n\gamma^2\theta\Psi}{(1+\theta^2\gamma^2+\Psi^2\gamma^2)} \end{aligned}\right\} \quad (2.14)$$

and the total emissivity integrated over all directions of emission is

$$\left.\begin{aligned} H &= \frac{4\pi^2 e^2 \Psi^2 \nu}{c} \sum_{n=1}^{\infty} \left[\{J_n'(v_n)\}^2 + w_m \{J_n(v_n)\}^2\right] \\ v_n &= \left\{\frac{\nu\gamma\Psi^2}{\nu_B}\left[2n - \frac{\nu\gamma\Psi^2}{\nu_B}\left(1 + \{\Psi\gamma\}^{-2}\right)\right]\right\}^{1/2} \\ w_n &= \left\{\frac{n - \frac{\nu\gamma\Psi^2}{\nu_B}(1+\{\Psi\gamma\}^{-2})}{v_n}\right\}^2 \end{aligned}\right\} \quad (2.15)$$

H is shown in Figure 3 for several values of $\Psi\gamma$.

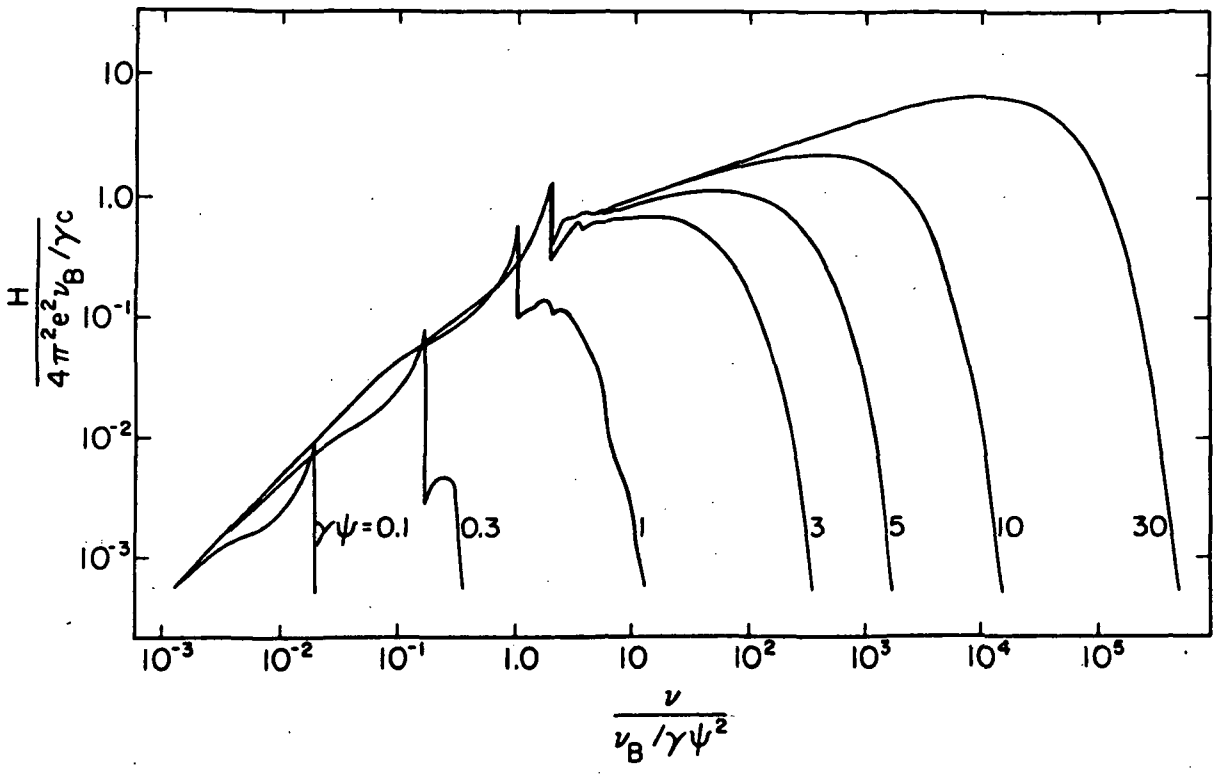

Fig. 3. The emissivity per unit frequency for relativistic particles which spiral with small pitch angles.

For very small pitch angles $\psi\gamma \ll 1$, equation (2.15) reduces to equation (2.10). When $\nu \gg \frac{\nu_B}{\gamma\psi^2}$, the approximations for Bessel functions of large order can be used in equation (2.15) yielding (Ginzburg and Syrovatskii, 1969)

$$H = \frac{2\pi\sqrt{3}\, e^2 \psi \nu_B}{c} \int_{\nu/\nu_c}^{\infty} K_{5/3}(x)\,dx \,, \qquad (2.16)$$

where $\nu_c = \frac{3}{2}\gamma^2\psi\nu_B$ and $K_{5/3}$ is the modified Bessel function of order 5/3.

For many computations such as the ones we will consider in Section IV the following simple approximations can be used.

For "Very-small-pitch-angle synchrotron radiation" $\gamma\psi < .6$

$$H = H_{(\text{equation } 10)} \ , \tag{2.17}$$

for "Small-pitch-angle synchrotron radiation" $\gamma\psi > .6$ and $\psi \ll 1$

$$H = \begin{cases} \dfrac{2\pi^2 e^2 \psi^2 \nu}{c} & , \quad \nu_B/\gamma \ll \nu < \nu_B/\gamma\psi^2 \\ H_{(\text{equation } 16)} \ , & \quad \nu_B/\gamma\psi^2 < \nu \end{cases} \ . \tag{2.18}$$

These approximations are accurate to about 1% when ν is less than $.1\ \nu_B/\gamma\psi^2$ or greater than $2\ \nu_B/\gamma\psi^2$. Large deviations (20% to 50%) only occur in the frequency range $.3 \leqslant \dfrac{\nu\gamma\psi^2}{\nu_B} < .8$ and only when $.5 \leqslant \gamma\psi \leqslant .8$.

In their study of low frequency cutoffs O'Dell and Sartori (1970b) assumed that H equals zero when $\nu < \dfrac{\nu_B}{\gamma\psi^2}$, $\psi \ll 1$ and $\gamma\psi \gg 1$; however, since $H \propto \nu$ is a more accurate approximation for this regime (equation 2.18), their conclusions (concerning the occurrence of a steep "cyclotron turnover") are incorrect. The actual emission spectra for source distributions of the type they considered are discussed in Example 2 of Section IV.

III. Synchrotron Radiation from Cosmic Sources: General Considerations

We will now consider the emission from optically thin synchrotron sources in which most of the radiating particles have small pitch angles. The formal expressions for the radiation from this type of source are easily found, but to use these expressions to compute observable quantities requires a complete description of the structure of the magnetic field and the particle distributions, information which in fact is never available. This difficulty can be circumvented if the source structure is amenable to certain approximations. Two approaches which can be taken are (1) one can first compute the radiation from a homogeneous source which is permeated by a uniform field and then make some allowances for the irregularities in the actual sources; or (2) one can at the outset assume that the magnetic field is tangled or irregular, and then assess how the results should be altered to account for a small degree of uniformity. The first approach is usually appropriate for conventional synchrotron sources, but when the emission is mainly from particles with small pitch angles, the second approach is likely to be more useful. In what follows we will discuss the conditions for which each of these approximation schemes are applicable and we will then derive expressions for the emission from sources in which the radiating particles have small pitch angles and the magnetic field structure is somewhat irregular.

First consider the emission from a small volume element in a synchrotron source. If the radiating particles mainly have small pitch angles, most of the emission will be concentrated within a small angle, θ_R, of the direction of the local magnetic field (θ_R is defined below in the text following equation 2.30). The magnitude of θ_R can be estimated as follows: For sources in which the characteristic pitch angle $\bar{\Psi}$ is large compared to the typical width of the radiation beam for the individual particles, $\bar{\gamma}^{-1}$, θ_R is of the order of $\bar{\Psi}$; but when $\bar{\Psi} \ll \bar{\gamma}^{-1}$, θ_R is fixed by the size of the individual radiation pattern. These estimates can be summarized as

$$\theta_R \approx \bar{\Psi} + \bar{\gamma}^{-1} . \qquad (2.19)$$

Now consider the source as a whole. The direction of the magnetic field will vary throughout the source and the magnitude of these variations can be characterized by an angle θ_B. By this we mean that the magnetic field through the source is aligned for the most part within θ_B of some given direction; if the field is absolutely uniform, θ_B is zero, and if it is very tangled, θ_B is of the order of unity (the precise definition for θ_B is given by equation 2.31, below). Figure 4 shows a schematic of a portion of a synchrotron source in which θ_B and θ_R are indicated. As before θ is the angle between the direction of observation and the direction of the local magnetic field.

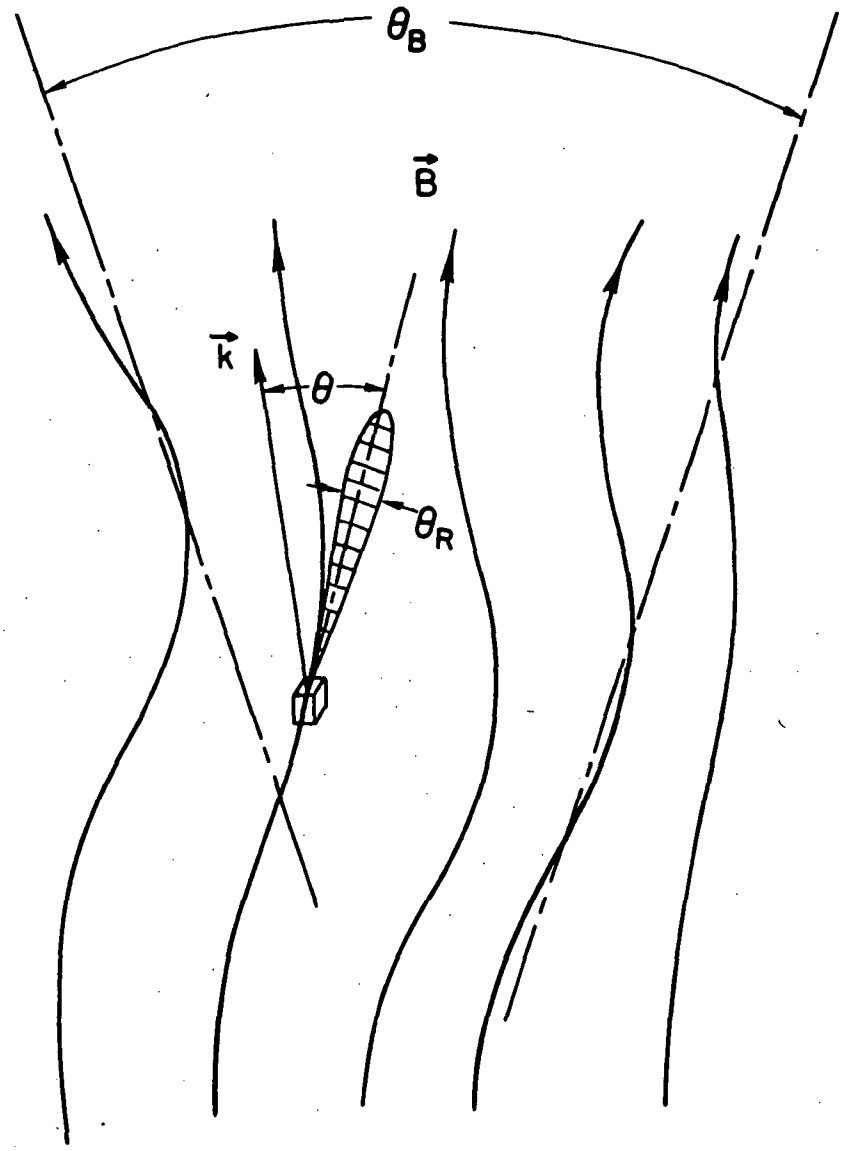

Fig. 4. The structure of a portion of a synchrotron source. The characteristic variation in the direction of the magnetic field, θ_B, is taken to be much greater than the width of the radiation pattern for the emission from a small volume element, θ_R.

When θ_R is much greater than θ_B, the variations in the direction of the magnetic field only broaden the radiation pattern by a small amount and the net emission from the source is only slightly altered by the irregularities in the magnetic field. In this case one

can compute the main features of the emission by assuming that the field is completely uniform. When $\theta_B \gg \theta_R$, however, the radiation from different regions of the source is beamed in widely different directions (relative to the size of the beam) so that the net emission in any one direction, say $\underset{\sim}{k}$, is proportional to the volume emissivity averaged over a number of the possible orientations of $\underset{\sim}{B}$ relative to $\underset{\sim}{k}$. Since the irregularities in the source structure are predominant in this case, the second approximation procedure can be used for computing the total source emission.

If a synchrotron source mainly contains particles with small pitch angles, then θ_R will be so small that even a moderate deviation from a strictly uniform magnetic structure will insure that $\theta_B \gg \theta_R$. Assuming that this condition is fulfilled we will now derive expressions for the emissivity and polarization of an optically thin source. The main results of these calculations can be anticipated as follows: (1) As we mentioned above, the net emission in the direction $\underset{\sim}{k}$ is the sum of the contributions from a number of regions in which $\underset{\sim}{B}$ has various orientations relative to $\underset{\sim}{k}$. This will enable us to express the total source emissivity, E, and the total emissivity of the circularly polarized radiation, E_c, in terms of the single particle emissivity integrated over all directions of emission (see equations 2.38 and 2.39, below). (2) Since the major axis of the polarization ellipse is in the $\underset{\sim}{k} \times \underset{\sim}{B}$ direction, its orientation varies for the emission from different regions of the source so that the total amount of linearly polarized radiation is relatively small; equation (2.42) gives an upper limit for the net degree of linear polarization. The remainder of this section

is concerned with deriving equations (2.38), (2.39) and (2.42); in the next section these results will be used to compute the emission for specific source models.

Let $n(\gamma,\psi,\underset{\sim}{r})\, d\gamma d\psi$ be the number of particles per unit volume at point $\underset{\sim}{r}$ with energies between γ and $\gamma + d\gamma$ and pitch angles between ψ and $\psi + d\psi$ $(0 \le \psi \le \pi/2)$. The emissivity of a single particle is expresses as $\eta(\nu,\theta,\psi,\gamma,B)$ so that for incoherent radiation the emissivity per unit volume in the $\underset{\sim}{k}$ direction and at frequency ν is

$$\epsilon(\nu,\underset{\sim}{k},\underset{\sim}{r}) = \int_1^\infty \int_0^{\pi/2} n\, \eta d\psi d\gamma \quad \text{erg(Hz sec str cm}^3\text{)}^{-1}. \tag{2.20}$$

Similarly, the volume emissivity of the circularly polarized radiation can be written as

$$\epsilon_c(\nu,k,r) = \int_1^\infty \int_0^{\pi/2} n\, \eta_c d\psi d\gamma\ , \tag{2.21}$$

where $\eta_c(\nu,\theta,\psi,\gamma,B) = \eta\rho_c$ and $\rho_c(\nu,\theta,\psi,\gamma,B)$ is the degree of circular polarization for the emission from an individual particle. The variable θ in the arguments of η and η_c is a function $\underset{\sim}{r}$ since it is the angle between $\underset{\sim}{k}$ and $\underset{\sim}{B}(r)$.

Assuming that the source is optically thin and that the ambient medium within the source does not significantly affect the transfer of the radiation we can express the total emissivity E and the circularly polarized emissivity E_c as

$$E_{(c)}(\nu,\underset{\sim}{k}) = \int_V \epsilon_{(c)} d^3r \quad \text{erg(Hz sec str)}^{-1} \tag{2.22}$$

where V is the total volume of the source or, if the source is sufficiently well resolved, the portion of the source which is being observed.

The degree of circular polarization is now given by

$$P_c(\nu,\underset{\sim}{k}) = E_c/E \quad . \tag{2.23}$$

If the quantities n and $\underset{\sim}{B}$ were known throughout the source, equation (2.22) could be used in its present form; however, since this is not normally the case, it would be more useful to have expressions which involve only the gross or average properties of the source. For the type of sources which we are considering here (ones for which θ_B is much greater than θ_R), these expressions can be obtained by changing the variables of integration in equation (2.22) and integrating over the orientations of the magnetic field.

The magnetic field at each point in the source can be expressed as

$$\underset{\sim}{B}(\underset{\sim}{r}) = B \sin\theta \cos\phi \; \underset{\sim}{i} + B \sin\theta \sin\phi \; \underset{\sim}{j} + B \cos\theta \; \underset{\sim}{k} \tag{2.24}$$

where $\underset{\sim}{i},\underset{\sim}{j},\underset{\sim}{k}$ form a set of three mutually perpendicular unit vectors, $\underset{\sim}{k}$ is in the direction of the observer, and B, θ and ϕ are functions of $\underset{\sim}{r}$. The volume element in equation (2.22) can be written in terms of the B, θ, ϕ variables by using

$$d^3r = \left| \frac{d^3r}{d^3B} \right| B^2 \, dB \sin\theta \, d\theta \, d\phi \quad . \tag{2.25}$$

This expression for d^3r represents that portion of the source volume in which the magnetic field strength is between B and $B + dB$ and the field direction is between θ and $d\theta$ in one of the angular

coordinates and between ϕ and $\phi + d\phi$ in the other.

By defining

$$N(\gamma,\Psi,B,\theta,\phi) \equiv n\left|\frac{d^3r}{d^3B}\right| B^2 \quad \text{particles (gauss str erg rad)}^{-1} \quad (2.26)$$

and using equation (2.25), we can transform equation (2.22) to

$$E_{(c)}(\nu,\underset{\sim}{k}) = \int N\, \eta_{(c)} \sin\theta\, d\theta\, d\phi\, dB\, d\Psi\, d\gamma \ . \quad (2.27)$$

The position $\underset{\sim}{r}$ in the argument of n in equation (2.26) is now a function of $\underset{\sim}{B}$. It may be that $\underset{\sim}{r}(\underset{\sim}{B})$ is not a single valued function of $\underset{\sim}{B}$, but this can be allowed for by modifying the definition of N as follows: Consider the source divided into, say, j regions, in each of which $\underset{\sim}{r}(\underset{\sim}{B})$ is a single valued function. The right hand side of equation (2.26) is evaluated separately in each of these regions, and N is taken to be the sum of these j terms.

The quantity N describes the net properties of a source. It gives the total number of particles which are in a given interval of energy and pitch angle and which are located in regions of the source in which the magnetic field has a certain range of directions and field strengths. Since we are concerned with sources in which the average pitch angle of the particles is small and the magnetic field is fairly irregular, N is peaked near $\Psi = 0$ and it is a slowly varying function of θ and ϕ. To simplify the analysis we will limit our discussion to sources for which N is separable

$$N(\gamma,\Psi,B,\theta,\phi) = \lambda(\gamma,B,\theta,\phi)\ \xi(\gamma,B,\Psi) \ . \quad (2.28)$$

With the definition

$$I_{(c)}(\nu,\theta,\Upsilon,B) \equiv \int_0^{\pi/2} \eta_{(c)}\xi \, d\Psi \ . \tag{2.29}$$

Equation (2.27) now becomes

$$E_{(c)}(\nu,\underset{\sim}{k}) = \int \lambda I_{(c)} \sin\theta \, d\theta \, d\phi \, dB \, d\Upsilon \ . \tag{2.30}$$

Since ξ is peaked in the vicinity of $\Psi = 0$ and η and η_c are small everywhere except for θ near Ψ and $\pi-\Psi$, the integrals I and I_c are peaked about $\theta = 0$ and $\theta = \pi$. Furthermore I and I_c are symmetric and antisymmetric functions of $(\theta-\pi/2)$, respectively (since η_c depends on the sign of $\underset{\sim}{k} \cdot \underset{\sim}{B}$ while η does not). A measure of the angular width of I is given by $\theta_R(\nu,\Upsilon,B)$, which we now define as the value of $\theta < \pi/2$ at which I is one half of its maximum value.

The overall structure of the source is described by λ. The quantity θ_B, which characterizes the scale of the irregularities in the source, is defined in terms of λ by

$$\theta_B(\Upsilon,B,\theta,\phi) \equiv \lambda \Big/ \left| \frac{\partial\lambda}{\partial\theta} \right| \ . \tag{2.31}$$

As we noted earlier, if the mean pitch angles of the relativistic particles in a synchrotron source is sufficiently small and if the magnetic field is somewhat irregular, then θ_B is much greater than θ_R. In the present context this means that λ is nearly constant over the ranges of the values of θ and ϕ for which I and I_c make

significant contributions to the integrands in equation (2.30). Therefore, by excluding λ from the angular integrations we only introduce relative errors of the order of (θ_R/θ_B). To this accuracy the expressions for E and E_c can be reduced to

$$E_{(c)}(\nu,\underset{\sim}{k}) = \int_0^\infty \int_1^\infty \{\lambda_{\theta=0} \overset{+}{(-)} \lambda_{\theta=\pi}\} Q_{(c)} d\gamma dB \qquad (2.32)$$

where

$$Q_{(c)}(\nu,\underset{\sim}{k},\gamma,B) \equiv \int_0^{2\pi}\int_0^{\pi/2} I_{(c)} \sin\theta \, d\theta \, d\phi = \int_0^{\pi/2}\int_0^{2\pi}\int_0^{\pi/2} \eta_{(c)} \xi \sin\theta \, d\theta \, d\phi \, d\psi \qquad (2.33)$$

and we have used the symmetries of I and I_c mentioned above.

Since $\xi(\gamma,B,\psi)$ is independent of θ and ϕ, Q and Q_c can be evaluated by first integrating over all directions of emission; this yields

$$Q_{(c)}(\nu,\gamma,B) = \int \xi \, H_{(c)} \, d\psi \, , \qquad (2.34)$$

where

$$H_{(c)}(\nu,\gamma,\psi,B) = \int \eta_{(c)} \sin\theta \, d\phi \, . \qquad (2.35)$$

H is given by equation (2.15) or it can be approximated by equations (2.17) and (2.18). For $\gamma\psi \ll 1$, H_c equals $H\rho_c(\nu)$ where $\rho_c(\nu)$ is given by equation (2.18). When $\nu \ll \nu_B/(\gamma\psi^2)$, H_c nearly equals $-\mu H$ (since this is mainly emission from the first harmonic and at large θ); and when $\gamma\psi \gg 1$ and $\nu \gg \nu_B/(\gamma\psi^2)$ H_c can be expressed as (Legg and

Westfold, 1968; Melrose, 1971b)*

$$H_c = \frac{4\pi\mu e^2 \nu_B}{\sqrt{3}\,c}\left[\int_{\nu/\nu_c}^{\infty} K_{1/3}(x)dx + 2\frac{\nu}{\nu_c}K_{1/3}\left(\frac{\nu}{\nu_c}\right)\right.$$

$$\left. - \frac{d}{d\Psi}\left(\tan\Psi\left\{\int_{\nu/\nu_c}^{\infty} K_{1/3}(x)dx + 2\frac{\nu}{\nu_c}K_{1/3}\left(\frac{\nu}{\nu_c}\right)\right\}\right)\right]; \qquad (2.36)$$

Combining equations (2.32) and (2.34) and the definitions

$$\begin{aligned} N_E(\gamma,\Psi,B,\underset{\sim}{k}) &\equiv \{\lambda_{\theta=0} + \lambda_{\theta=\pi}\}\,\xi(\gamma,B,\Psi) \\ N_c(\gamma,\Psi,B,\underset{\sim}{k}) &\equiv \{\lambda_{\theta=0} - \lambda_{\theta=\pi}\}\,\xi(\gamma,B,\Psi) \end{aligned} \qquad (2.37)$$

we obtain our final expressions for the source emissivities

$$E(\nu,\underset{\sim}{k}) = \int_0^{\infty}\int_1^{\infty}\int_0^{\pi/2} N_E H\, d\Psi\, d\gamma\, dB \qquad (2.38)$$

$$E_c(\nu,\underset{\sim}{k}) = \int_0^{\infty}\int_1^{\infty}\int_0^{\pi/2} N_c H_c\, d\Psi\, d\gamma\, dB\,. \qquad (2.39)$$

Equations (2.38) and (2.39) give the emission and degree of circular polarization in the $\underset{\sim}{k}$ direction in terms of the functions N_E and N_c,

*Integration of equation (2.34) by parts yields the integrand

$$\frac{4\pi\mu e^2 \nu_B \xi}{\sqrt{3}\,c}\left[\left(1 + \frac{\tan\Psi}{\xi}\frac{d\xi}{d\Psi}\right)\int_{\nu/\nu_c}^{\infty} K_{1/3}(x)dx + 2\frac{\nu}{\nu_c}K_{1/3}\left(\frac{\nu}{\nu_c}\right)\right].$$

When ξ is replaced by $\phi(\Psi)\sin\Psi/2$, this expression can be written as $8\pi^2 i\, \varepsilon^{21}(E,\omega,\Psi)\sin\Psi$ where ε^{21} is given by equation 37 of Melrose (1971b).

which describe the net properties of those portions of the source in which the magnetic field is parallel to $\underset{\sim}{k}$, and in terms of the functions H and H_c, which describe the average contribution of each particle to the total emission. N_E represents the total flux of particles in the direction of the observer; while N_c is equal to the particle flux in the regions in which $\underset{\sim}{B} \cdot \underset{\sim}{k}$ is positive minus the particle flux in the regions in which $\underset{\sim}{B} \cdot \underset{\sim}{k}$ is negative.

While it was possible to express the circularly polarized emissivity simply as an integral of $N_c H_c$, a similar expression cannot be obtained for the linearly polarized emissivity, because, for the type of source with which we are concerned here $(\theta_B > \theta_R)$, the degree and direction of linear polarization depends very sensitively on the magnetic field structure; nevertheless, we can still set an upper limit to the degree of linear polarization. First consider the emission from a source for which $N(\gamma,\Psi,B,\theta,\phi)$ is isotropic. Since there is no preferred direction along which the polarization ellipse could be aligned, the degree of linear polarization for this emission must be zero. For the more general cases where the source distribution can be described by the sum of an isotropic term, N_o, and a non-isotropic term, N_1, the emission which is related to N_o will not exhibit any linear polarization, while the emission from the portion of the source which is represented by N_1 will, in general, be somewhat linearly polarized. In the vicinity of $\theta = 0$ the total source distribution function can be expressed as

$$\left.\begin{aligned} N(\gamma,\Psi,B,\theta,\phi) &= N_o(\gamma,\Psi,B) + N_1(\gamma,\Psi,B,\theta,\phi) \\ N_o &= N(\gamma,\Psi,B,\theta=0) \\ N_1 &= \theta \times \left[\lim_{\theta \to 0} \frac{\partial N}{\partial \theta}\right] . \end{aligned}\right\} \qquad (2.40)$$

The source distribution function near $\theta = \pi/2$ can be expanded in the same way, but to simplify the present discussion the contributions from these terms will not be included here.

The total emissivity for the source, E, and the emissivity for the anisotropic portion of the source distribution, E_1, are given by equation (2.27), and the angular derivative of N is related to θ_B by equation (2.31) so that an upper limit to the degree of linear polarization can be written as

$$P_\ell(\nu,\underset{\sim}{k}) \leqslant \frac{E_1(\nu,\underset{\sim}{k})}{E(\nu,\underset{\sim}{k})} = \frac{\int(\theta/\theta_B)N\eta \sin\theta \, d\theta \, d\phi \, dB \, d\Psi \, d\gamma}{\int N\eta \sin\theta \, d\theta \, d\phi \, dB \, d\Psi \, d\gamma} \quad . \tag{2.41}$$

Since the integrands in equation (2.41) are small everywhere except for $\theta \leqslant \theta_R$, the upper limit for P_ℓ becomes

$$P_\ell(\nu,\underset{\sim}{k}) \leqslant \theta_R/\theta_B \ll 1 \quad . \tag{2.42}$$

For sources in which the relativistic particles have small pitch angles and the magnetic field is somewhat non-uniform, the radiation will exhibit only a small degree of linear polarization; the actual amount will depend on the details of the source structures and particle distributions. For these reasons we cannot derive any useful quantitative expressions for the linear polarization and have not attempted to compute the degrees of linear polarization for the simple source models considered in the next section.

IV. Synchrotron Sources: Examples

We will consider the emission from source distributions of the form

$$N_{\binom{E}{c}}(\gamma,\Psi,B,\underset{\sim}{k}) = \binom{+1}{\mu}\begin{cases} G\,\gamma^{-s}\Psi\,\exp[-\Psi^2/\tilde{\Psi}^2]\delta(B-B_o) & \gamma_1 < \gamma < \gamma_2 \\ 0 & \text{otherwise} \end{cases} \tag{2.43}$$

where $\gamma_1 \gg 1$, $\tilde{\Psi} \ll 1$ and $s > 1$. The dependence of N_E and N_c on $\underset{\sim}{k}$ is not explicitly shown, but the parameters $G, s, \tilde{\Psi}, B_o, \gamma_1$ and γ_2 may be slowly varying functions of $\underset{\sim}{k}$. The sources described by these distributions have (1) energy spectra which follow power laws within certain intervals and are zero elsewhere and (2) pitch angle distributions which are peaked at small angles. We have assumed that the magnetic field can be characterized by a single value of the field strength and that $\mu \equiv (-e\,\underset{\sim}{B}\cdot\underset{\sim}{k})$ is everywhere of the same sign.

The source emissivity and the degree of circular polarization for a given distribution function are obtained by using equations (2.23), (2.38) and (2.39). We have computed these quantities for three sets of parameters: (1) $\gamma_2\tilde{\Psi} \ll 1$, (2) $\gamma_1\tilde{\Psi} \gg 1$, and (3) $\gamma_1\tilde{\Psi} \ll 1$ and $\gamma_2\tilde{\Psi} \gg 1$. These examples illustrate sources which predominately emit very-small-pitch-angle synchrotron radiation (equation 2.17), small-pitch-angle synchrotron radiation (equation 2.18), and a combination of the two, respectively.

EXAMPLE 1. $\gamma_2\tilde{\Psi} \ll 1$: Very-Small-Pitch-Angle Synchrotron Radiation

These distribution functions describe sources in which essentially all of the particles have $\gamma\Psi \ll 1$. The appropriate single particle emissivities are H as given by equation (2.17) and $H_c = \rho_c(\nu)$ is given by the last expression in equation (2.8). The source emissivity and the degree of circular polarization are

$$\underset{\sim}{E}(\nu,k) = A(\gamma_2\tilde{\Psi})^{2-s} \times \begin{cases} \frac{\nu}{\nu_2}\left\{\left(\frac{\nu_2}{\nu_1}\right)^{s-1}\left[\frac{1}{s-1} - \frac{2}{s}\frac{\nu}{\nu_1} + \frac{2}{s+1}\left(\frac{\nu}{\nu_1}\right)^2\right] \right. \\ \qquad \left. - \left[\frac{1}{s-1} - \frac{2}{s}\frac{\nu}{\nu_2} + \frac{2}{s+1}\left(\frac{\nu}{\nu_2}\right)^2\right]\right\} & \nu_B/\gamma_1 \ll \nu < \nu_1 \\ \left(\frac{\nu}{\nu_2}\right)^{2-s}\left\{\left[\frac{1}{s-1} - \frac{2}{s} + \frac{2}{s+1}\right]\right. \\ \left. -\left(\frac{\nu}{\nu_2}\right)^{s-1}\left[\frac{1}{s-1} - \frac{2}{s}\frac{\nu}{\nu_2} + \frac{2}{s+1}\left(\frac{\nu}{\nu_2}\right)^2\right]\right\} & \nu_1 < \nu < \nu_2 , \end{cases} \tag{2.44}$$

$$P_c(\nu,k) = \frac{\mu A(\gamma_2\Psi)^{2-s}}{\underset{\sim}{E}(\nu,k)} \begin{cases} \frac{\nu}{\nu_2}\left\{\left(\frac{\nu_2}{\nu_1}\right)^{s-1}\left[\frac{2}{s}\frac{\nu}{\nu_1} - \frac{1}{s-1}\right] - \left[\frac{2}{s}\frac{\nu}{\nu_2} - \frac{1}{s-1}\right]\right\} & \nu_B/\gamma_1 \ll \nu < \nu_1 \\ \left(\frac{\nu}{\nu_2}\right)^{2-s}\left\{\left[\frac{2}{s} - \frac{1}{s-1}\right] - \left(\frac{\nu}{\nu_2}\right)^{s-1}\left[\frac{2}{s}\frac{\nu}{\nu_2} - \frac{1}{s-1}\right]\right\} & \nu_1 < \nu < \nu_2 , \end{cases} \tag{2.45}$$

where $A \equiv (2\pi^2 e^2 \nu_B G\, \tilde{\Psi}^{s+2})/c$, ν_B is evaluated at $B = B_o$, $\nu_1 = 2\gamma_1\nu_B$, $\nu_2 = 2\gamma_2\nu_B$ and s is not exactly equal to 2. The functions E and P_c are shown in Figure 5 for $\gamma_1\tilde{\Psi} = 10^{-4}$ and $\gamma_2\tilde{\Psi} = .1$.

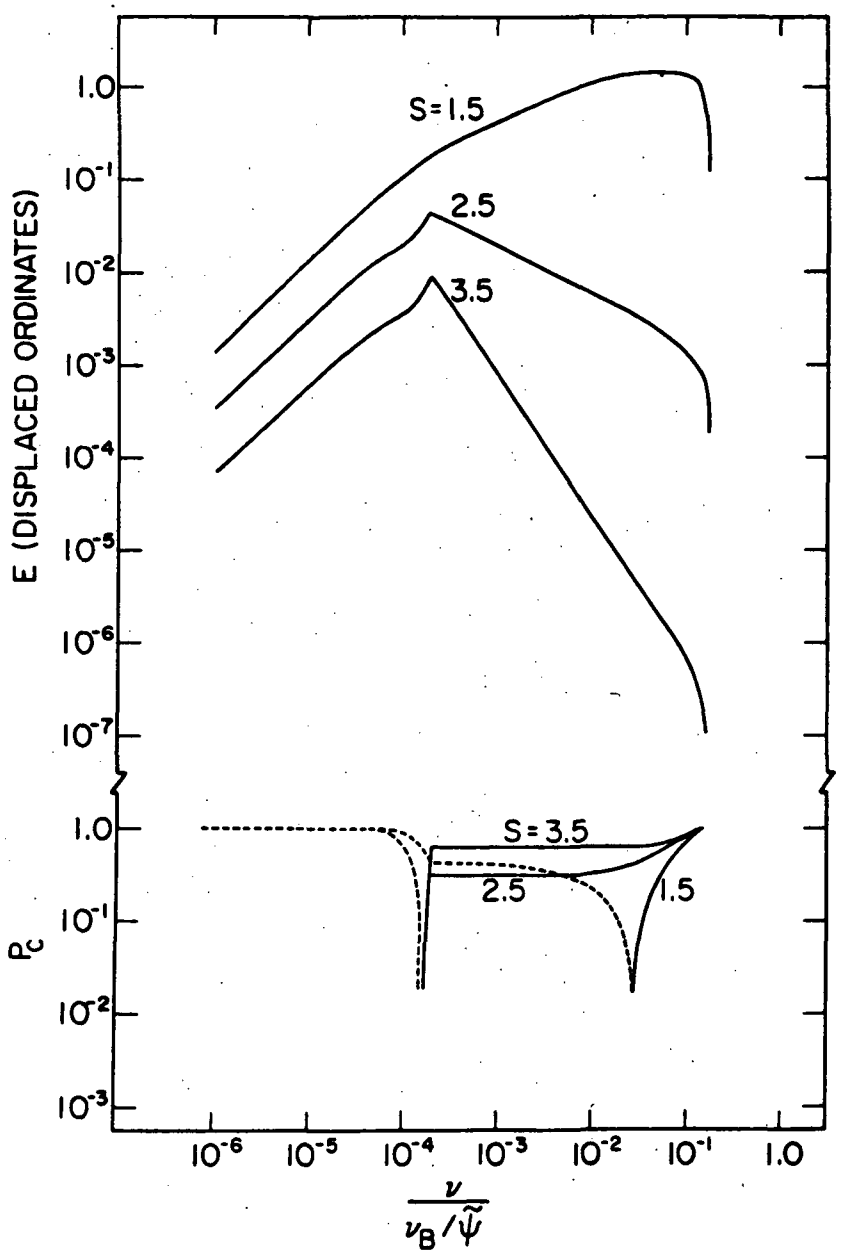

Fig. 5. The source emissivity and the degree of circular polarization: Example 1; $\gamma_1\tilde{\Psi} = 10^{-4}$; $\gamma_2\tilde{\Psi} = .1$. The solid and dotted P_c curves indicate opposite sense of circular polarization.

The spectra are mainly composed of two regions: a high frequency region where

$$\left.\begin{aligned} \nu_1 &\ll \nu \ll \nu_2 \\ E &\propto \nu^{2-s} \\ P_c &\approx \mu \frac{(s-2)(s+1)}{s^2-s+2} \end{aligned}\right\} \qquad (2.46)$$

and a low frequency region where

$$\left.\begin{aligned} \nu_B/\gamma_1 &\ll \nu \ll \nu_1 \\ E &\propto \nu \\ P_c &\approx -\mu \ . \end{aligned}\right\} \qquad (\ .57)$$

At the higher frequencies the spectra follow power laws, but the power law indices differ from that which is obtained by conventional synchrotron theory; in the present case the logarithmic slope of the emissivity is $2-s$ instead of the usual result of $(1-s)/2$.

From Figure 5 it can be seen that the sense of the circular polarization reverses near the frequency at which the emission is a maximum. This is a striking feature by which it may be possible to identify this type of emission; however, there are other processes whereby similar effects can be produced. Several authors (Ramaty, 1969; Pacholczyk and Swihart, 1970; Melrose, 1971b) have noted that synchrotron sources which are self absorbed at low frequencies may also exhibit a reversal in the sense of the circular polarization. If a reversal of this sort were ever observed, it would be necessary to rely on other features of

the emission, such as the shape of the spectrum and the variations of the polarization with frequency, to distinguish between self absorption and the optically thin emission considered here.

Recently Tademaru (1972) and Melrose (1971a) have studied the emission from particles with very small pitch angles ($\gamma\Psi \ll 1$). Tademaru's work was concerned with the emission from distributions which are significantly different from those considered in the present investigation. Melrose computed the quantities r_ℓ and r_c which, in the present notation, are equivalent to

$$r_{\ell,c} = \frac{\int_0^\infty \rho_{\ell,c}(\nu) H \, d\nu}{\int_0^\infty H \, d\nu} \tag{2.48}$$

where ρ_ℓ, ρ_c and H are given by equations (2.8), (2.9) and (2.10), respectively. It is not clear how r_ℓ and r_c can be related to observable quantities. Melrose claimed that $|r_c|$, which equals .5, represents an upper limit to the degree of circular polarization which can be exhibited by a source; however, as one can see from Figure 5, this clearly is not true.

EXAMPLE 2. $\gamma_1\tilde{\Psi} \gg 1$: Small-Pitch-Angle-Synchrotron Radiation

For sources described by these distribution functions most of the particles have $\gamma\Psi \gg 1$ and $\Psi \ll 1$ so that the single particle emissivity, H, can be approximated by equation (2.18). At high frequencies the function H_c is given by equation (2.36) and at very low frequencies it is equal to $-H$. In those frequency intervals for which

equations (2.38) and (2.39) can be easily evaluated the source emissivity and the degree of circular polarization are given by

$$E(\nu,\underset{\sim}{k}) = A \times \begin{cases} c_1(\gamma_1\tilde{\Psi})^{1-s}\,\dfrac{\nu\tilde{\Psi}}{\nu_B} & \dfrac{\nu_B}{\gamma_1} \ll \nu \ll \dfrac{\nu_B}{\gamma_1\tilde{\Psi}^2} \\ c_2(\gamma_1\tilde{\Psi})^{1/3-s}\left(\dfrac{\nu\tilde{\Psi}}{\nu_B}\right)^{1/3} & \dfrac{\nu_B}{\gamma_1\tilde{\Psi}^2} \ll \nu \ll \nu_B\gamma_1^{\,2}\tilde{\Psi} \\ c_3\left(\dfrac{\nu\tilde{\Psi}}{\nu_B}\right)^{\frac{1-s}{2}} & \nu_B\gamma_1^{\,2}\tilde{\Psi} \ll \nu \ll \nu_B\gamma_2^{\,2}\tilde{\Psi} \end{cases} \qquad (2.49)$$

$$P_c(\nu,\underset{\sim}{k}) = \mu \times \begin{cases} -1 & \dfrac{\nu_B}{\gamma_1} \ll \nu \ll \dfrac{\nu_B}{\gamma_1\tilde{\Psi}^2} \\ c_4(\gamma_1\tilde{\Psi})^{-5/3}\left(\dfrac{\nu\tilde{\Psi}}{\nu_B}\right)^{1/3} & \dfrac{\nu_B}{\gamma_1\tilde{\Psi}^2} \ll \nu \ll \nu_B\gamma_1^{\,2}\tilde{\Psi} \\ c_5\left(\dfrac{\nu\tilde{\Psi}}{\nu_B}\right)^{-1/2} & \nu_B\gamma_1^{\,2}\tilde{\Psi} \ll \nu \ll \nu_B\gamma_2^{\,2}\tilde{\Psi} \end{cases} \qquad (2.50)$$

The functions $c_i(s)$ are defined and tabulated in the Appendix. The quantities E and P_c are shown in Figure 6 for $\gamma_1\tilde{\Psi} = 10$ and $\gamma_2\tilde{\Psi} > 10^3$. For frequencies much higher than $\nu_B/\gamma_1\tilde{\Psi}^2$ our results for the source emissivity and the polarization are the same as those of conventional synchrotron theory (Ginzburg and Syrovatskii, 1965; Legg and Westfold, 1968). At frequencies lower than $\nu_B/\gamma_1\tilde{\Psi}^2$, however, the emission decreases linearly with frequency and becomes strongly circularly polarized. O'Dell and Sartori (1971b) were the first to note that synchrotron spectra should have unusual features in this frequency range; however, their actual analysis was incorrect because, as we mentioned in Section II, they used a poor approximation for the single particle emissivity.

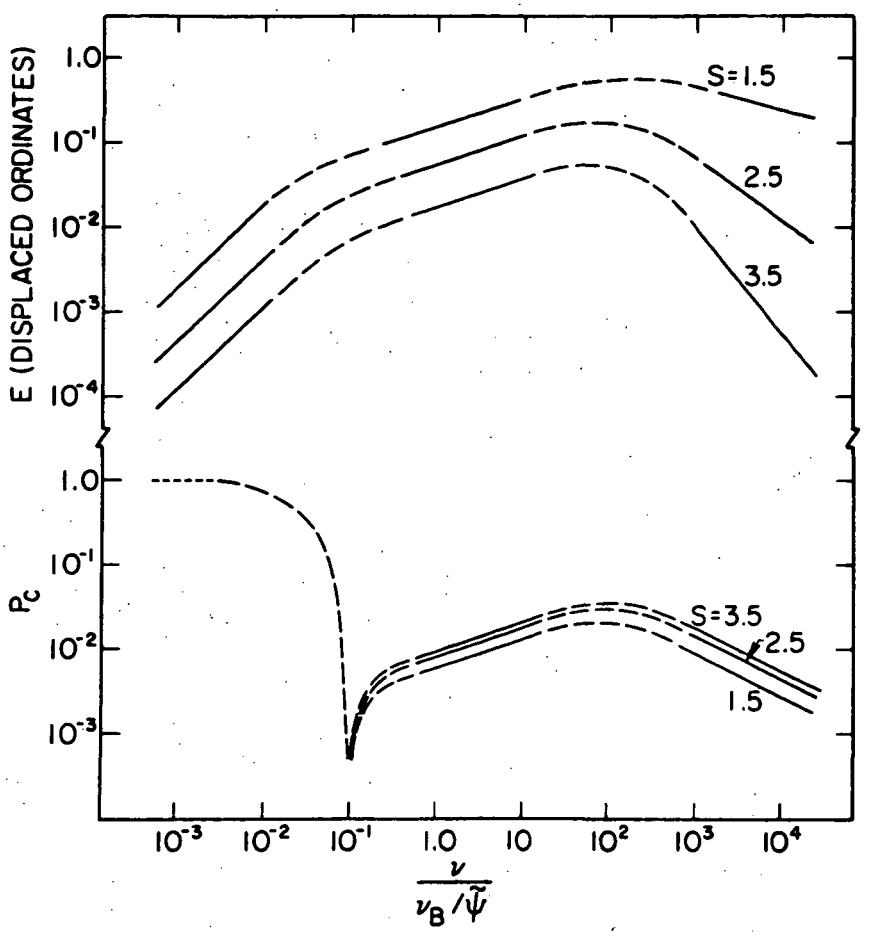

Fig. 6. Same as Figure 5: Example 2; $\gamma_1\tilde{\Psi} = 10$; $\gamma_2\tilde{\Psi} > 10^3$. The dashed curve segments are rough interpolations between the computed portions of the curves.

EXAMPLE 3. $\gamma_1\tilde{\Psi} \ll 1$ and $\gamma_2\tilde{\Psi} \gg 1$: Small-Pitch-Angle and Very-Small-Pitch-Angle Synchrotron Radiation

These distributions are essentially superpositions of the distributions of Examples 1 and 2. At low frequencies the emission is similar to that of Example 1 and at high frequencies it is similar to that of Example 2. For intermediate frequencies, $\nu \approx \nu_B/\tilde{\Psi}$, the spectra are either concave or convex (on a log E versus log ν display) for

distribution indices s greater or less than 3, respectively. The emissivity and degree of circular polarization for this example are shown in Figure 7 where $\gamma_1\tilde{\Psi} = 10^{-3}$ and $\gamma_2\tilde{\Psi} > 10^3$.

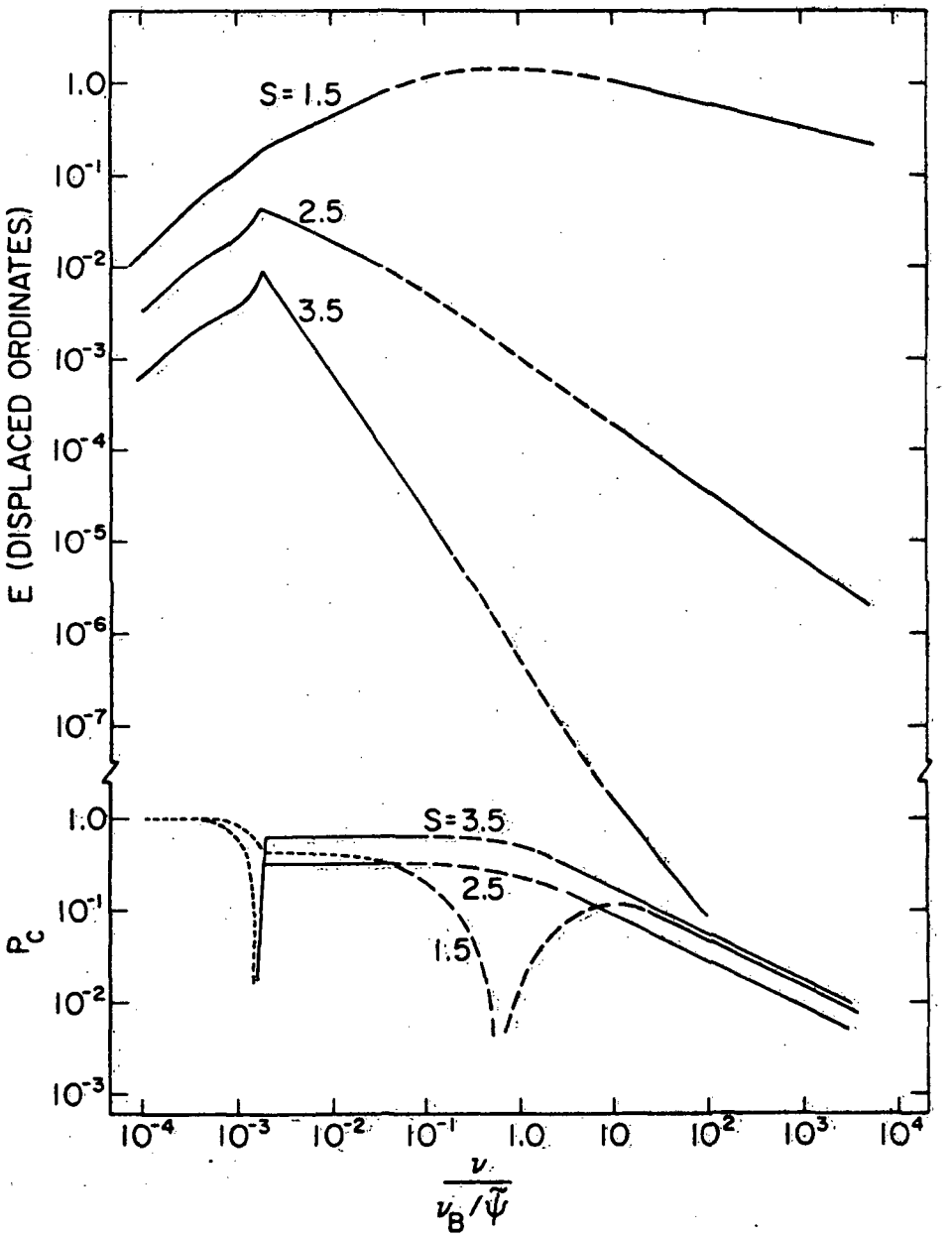

Fig. 7. Same as Figure 6; Example 3; $\gamma_1\tilde{\Psi} = 10^{-3}$; $\gamma_2\tilde{\Psi} > 10^3$.

V. Summary

The emission from a relativistic particle which spirals with a small pitch angle ($\Psi \lesssim \gamma^{-1}$) differs qualitatively from the usual synchrotron emission ($\Psi \gg \gamma^{-1}$): the particle spectrum peaks around $\nu \approx \gamma\nu_B$ (instead of at $\nu \approx \gamma^2 \sin\Psi\ \nu_B$) and falls off linearly with frequency as $\nu \to 0$ (rather than as $\nu^{1/3}$). For sources which mainly contain particles with small pitch angles, the degree of circular polarization will normally be high, whereas, if the magnetic field is somewhat irregular, the degree of linear polarization will be small. If the particle distribution also has a low energy cutoff, the emissivity will vary linearly with frequency at low frequencies. Applications of these results to specific astrophysical problems are considered in Chapter 3.

Chapter 3

MODELS OF SOME COSMIC SOURCES

I. Introduction

Recent measurements of polarization, angular structure and variability allow us to place some constraints on the possible synchrotron models for the radiation from pulsars and extragalactic objects. Using the conventional theory for synchrotron emission and the extension of this theory for particles with small pitch angles (Chapter 2), we have examined the plausibility of several models for the optical emission from the pulsar NP 0532, and for the low frequency cutoffs in the radio emission from PKS 2134 + 004 and OQ 208 and in the infrared emission from NGC 1068.

II. Optical Radiation from NP 0532

Several authors (Shklovsky, 1970; Sturrock, 1971; O'Dell and Sartori, 1970b; Zheleznyakov, 1971; and Lerche, 1970) have suggested that the optical radiation from the Crab Nebula pulsar is due to electron synchrotron radiation. O'Dell and Sartori (1970a) noted that some of these models were invalid because the authors failed to take into account the range of energies and pitch angles for which the conventional formulation of synchrotron theory is valid. We have extended their arguments by including the time variations and the polarization of the emission. The additional restrictions which we have derived rule out models for the optical emission for NP 0532 which involve incoherent electron synchrotron emission from regions within the velocity-of-light cylinder.

The temporal structure of the optical pulses is presumably due to the "searchlight effect": the pulsar emits a narrow beam of radiation which corotates with the star and sweeps past the direction of the observer during each rotation. In this picture, the observed variations in the intensity correspond to features in the angular structure of the pulsar beam. The optical radiation from NP 0532 varies very rapidly when the intensity is near its maximum value; changing from increasing to decreasing intensity so abruptly that the peak appears cusp-like when measured with a resolution of 32 μsec (Papaliolios, et al., 1970). Since the period of the Crab nebula pulsar is 33 msec, the variations imply that the pulsar beam has angular structure of less than $2\pi \times (32\ \mu\text{sec})/(33\ \text{msec}) \approx 6 \times 10^{-3}$ radians.

For a collection of relativistic electrons streaming along a magnetic field the smallest structure in the synchrotron radiation pattern is greater than either the characteristic value of the pitch angle $\bar{\Psi}$ or the reciprocal of the characteristic normalized energy, $\bar{\gamma}^{-1}$ (see equations 2.7 and 2.14). An electron of energy γmc^2 and pitch angle Ψ mainly radiates near the frequency $\nu \approx \nu_B \times \max\{3/2\ \gamma^2 \sin\Psi,\ 2\gamma\}$ (equations 2.10 and 2.16). These two relations and the observation that the optical radiation pattern (frequency $\sim 6 \times 10^{14}$) has structure smaller than 6×10^{-3} radians, yields two conditions which must be satisfied for electron synchrotron radiation:

$$B \leq 6.4 \times 10^5 \text{ gauss} , \tag{3.1}$$

$$\bar{\gamma}\,\bar{\Psi} \leq \left[\frac{8.5 \times 10^5 \text{ gauss}}{B}\right]^{1/2} . \tag{3.2}$$

The upper limit value of 6.4×10^5 gauss is near the lower limit of the magnetic field strength in the corotating portion of the magnetosphere of the Crab Nebula pulsar. If the pulsar is a neutron star of radius 10^6 cm which is threaded by a dipolar magnetic field, then a strength of 10^{12} gauss at the stellar surface implies a field strength of 1.5×10^5 gauss at the velocity-of-light cylinder. Closer in, where the magnetic field is more intense, equation (3.1) indicates that there cannot be any optical electron synchrotron emission (cf. Sturrock, 1971). Since the magnetosphere cannot corotate with the star beyond the velocity-of-light-cylinder it is difficult to understand how the beaming of the emission could be produced; however, it has been suggested that pulsed synchrotron emission from this region might result from interaction of

the low frequency electromagnetic waves from the pulsar with a surrounding plasma (Lerche, 1970). In this region, the magnetic field strength is much weaker so that equations (3.1) and (3.2) are not important constraints.

For pulsar models in which optical synchrotron radiation emanates from a region near the velocity-of-light cylinder (Shklovsky, 1970; O'Dell and Sartori, 1970b), equation (3.2) indicates that the product $\bar{\gamma}\,\bar{\psi}$ must be of the order of unity. Since the degree of circular polarization for synchrotron radiation from a relativistic particle is of the order of $(\gamma \sin \psi)^{-1}$ (Legg and Westfold, 1968; equation 2.8), this emission should exhibit a high degree of circular polarization. While the linear polarization of the optical radiation has been observed to be strong, varying from 0% to 26% in the course of each pulse (Cocke, et al., 1970), the circular polarization is less than about 1% during all phases of the pulse (Cocke, et al., 1971). There does not seem to be any simple way to reconcile the lack of detectable circular polarization with any of the current models which suggest that the optical radiation is due to incoherent electron synchrotron emission from the corotating portion of the pulsar magnetosphere.

The limit on the magnetic field in equation (3.1) will be less restrictive ($B \leqslant 10^9$ gauss) for synchrotron emission by protons. Furthermore, the low observed circular polarization would be consistent with emission by equal numbers of electrons and positrons near the velocity-of-light cylinder. Models of these types need more detailed investigation.

III. Low Frequency Cutoffs in Synchrotron Spectra

A number of cosmic sources have emission spectra which peak at radio or infrared frequencies. For frequencies above the peaks where these spectra can often be approximated by power laws (flux density $\propto \nu^{-\alpha}$) the emission is most readily interpreted as synchrotron radiation from optically thin power law distributions of electrons (number per energy interval $\propto$ (energy)$^{-s}$; $s = 2\alpha + 1$); however, it is not clear which of several possible explanations of the low frequency cutoffs is most reasonable for any given source. It is often assumed that the low frequency emission is suppressed by synchrotron self absorption; but the high degree of circular polarization which is measured from some objects is inconsistent with this interpretation (Berge and Seielstad, 1972) and the shape of some spectra is not that which would expected from a simple synchrotron self absorption model. In this section we examine the possibility that the peaked spectra are produced by emission from electron distributions which have low energy cutoffs and small average pitch angles and compare the predictions of this type of model with those of models which involve synchrotron self absorption or absorption by a thermal plasma. We shall consider three sources: the quasar PKS 2134 + 004 and the Seyfert galaxies OQ 208 and NGC 1068. The observational data for these objects have been compiled in Table 1 and Figures 8 and 9.

TABLE 1 - OBSERVATIONS

Source	PKS 2134 + 004	OQ 208	NGC 1068
z	1.93 [a]	.077 [b]	.0041 [c]
θ (seconds of arc)	.0007 ± .001 [d]	.0018 ± .0003 [e]	< 3.0 [f]
P_ℓ (%)	1.9 ± .8 [a]	--	.56 [g]
P_c (%)	.43 ± .08 [h]	--	< .05 [j]
t_v (years)	≥ 15 [k]	≥ 11 [k]	1.5 [ℓ]
F_{opt}(erg $sec^{-1}Hz^{-1}cm^{-2}$)	$\sim 2.5 \times 10^{-27}$ [a]	10^{-25} [b]	see Fig. 9
F_x(erg $sec^{-1}Hz^{-1}cm^{-2}$)	--	--	$< 2 \times 10^{-28}$ [m]

The symbols used in column 1 are as follows: z is the redshift; θ is the angular diameter; P_ℓ and P_c are the degrees of linear and circular polarization, respectively; $t_v \equiv F/(dF/dt)$ is the characteristic time scale for intensity variations; F_{opt} is the optical flux ($\nu \approx 6 \times 10^{14}$Hz); and F_x is the x-ray flux ($\nu \approx 7.5 \times 10^{17}$Hz). For the quantities θ and t_v we have listed the measurements which were made nearest the frequency of the peaks in the spectra.

a. Shimmins et al. (1968).

b. Blake et al. (1970).

c. Burbidge et al. (1959).

d. Broderick et al. (1971). This measurement was made at 5 GHz. At 2.3 GHz the diameter is ".0015 ± ".0002 (Kellermann et al., 1970).

e. Kellermann et al. (1970).

f. Neugebauer et al. (1971).

g. Kruszewski (1968). P_ℓ was measured at 3.18×10^{14}Hz.

h. Roberts et al. (1972). This was observed at 1.42 GHz; at 1.39 GHz $P_c = +0.28 \pm 0.035\%$ and at 5 GHz, $P_c = 0.13 \pm 0.009\%$.

j. Kemp et al. (1972). This limit was found for the optical emission.

k. Andrew et al. (1972) and Medd et al. (1972).

ℓ. Kleinmann and Low (1970), Low and Rieke (1971) and Rieke and Low (1972).

m. Gursky et al. (1971).

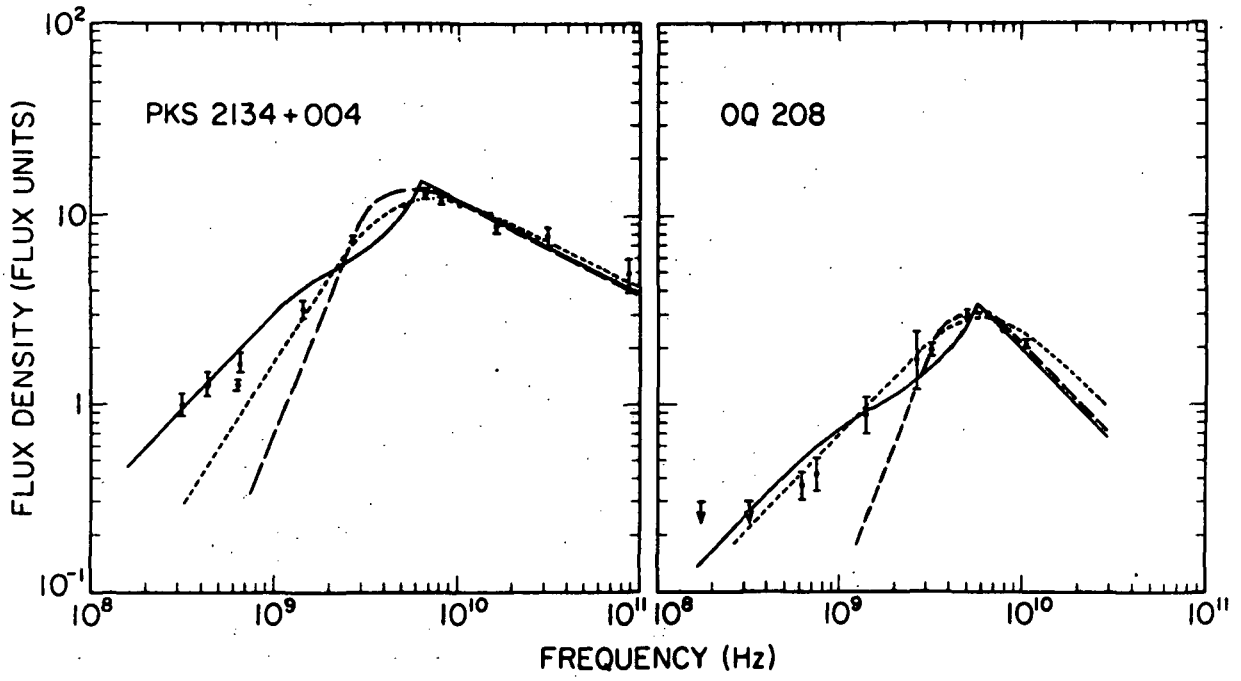

Fig. 8. Spectra for PKS 2134 + 004 and OQ 208. The absence of error bars for some of the points indicates that the uncertainties are comparable to the size of the dot. The solid curves are for the small-pitch-angle models; the dashed curves are the theoretical spectra for a single, homogeneous, self-absorbed source; and the dotted curves are for the thermal-absorption model. The references for the data are as follows: Blake, 1970 (.178 and 5 GHz); Cohen et al., 1971 (7.89 GHz); Jauncey et al., 1970 (818 and 606 MHz); Kellermann and Pauliny-Toth, 1971 (5, 10, 15, 31, and 86 GHz); Kraus and Andrew, 1970 (1.42, 2.65, 3.2, 6.6 and 10.6 GHz); Shimmins et al., 1968 (.47, .64, 1.41, 2.65, 6.5, 8.6, 10.5, and 16.2 GHz).

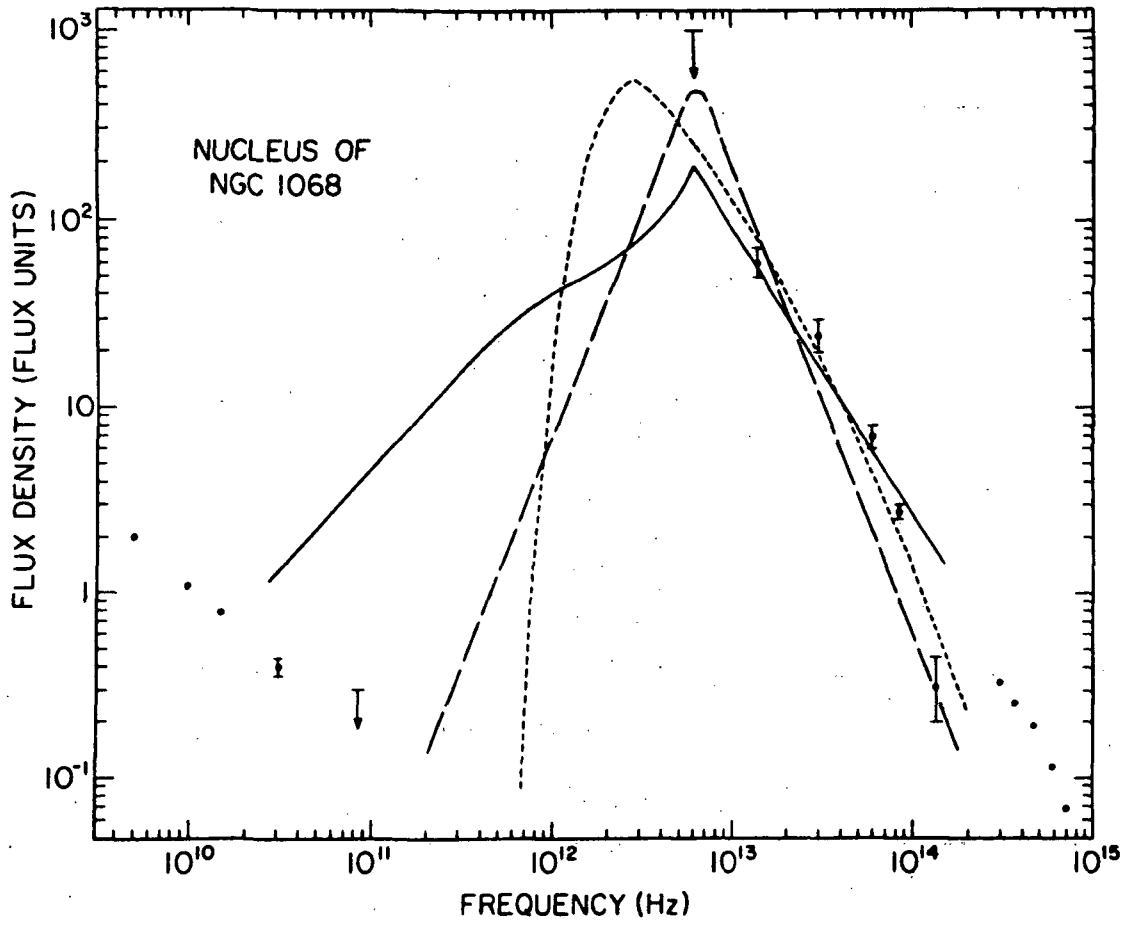

Fig. 9. Spectrum for the nucleus of NGC 1068. The curves and data points are interpreted as in Figure 1. The references for the data are: Kellermann and Pauliny-Toth, 1971 (5, 10, 15, 31, and 86 GHz); Rieke and Low, 1972 (6×10^{12}Hz); Kleinmann and Low, 1970 (1.36, 3, 6, 8.82, 13.6×10^{13}Hz); Kruszewski, 1968 (3.18, 3.36, 4.68, 5.79, and 6.99×10^{14}Hz).

A) Small-Pitch-Angle Models

It is well known that in a vacuum an isotropic distribution of relativistic electrons cannot produce a synchrotron spectrum which is steeper than $\nu^{1/3}$; however, in Chapter 2 it was shown that for a particle distribution for which the characteristic pitch angle is sufficiently small ($\bar{\Psi} \leq \bar{\gamma}^{-1}$) and which has a low energy cutoff the

emissivity may vary almost linearly with frequency and show a high degree of circular polarization. This result raises the possibility that a linear low frequency falloff in spectra in conjunction with a high degree of circular polarization might be a consequence of just this form of electron distribution rather than any absorption process.

The notion that relativistic electrons may be streaming with small pitch angles relative to the magnetic field has already been incorporated in some models of quasars (Woltjer, 1966; Noerdlinger, 1969), although pitch angles as small as $\bar{\gamma}^{-1}$ were not considered. There are several reasons why one might expect streaming of the relativistic particles in compact extragalactic objects. Small pitch angles might result from a plasma process which preferentially accelerates particles in the direction of the magnetic field (Speiser, 1965). They might also be produced while the particles traverse the nucleus of the galaxy. Observations of variable radio sources give evidence for presence of expanding clouds of relativistic particles. In previous studies (e.g. Kellermann and Pauliny-Toth, 1968) it has been assumed that a randomly oriented magnetic field permeates the cloud and expands with it. However, if such clouds are injected into regions where the magnetic field has an open configuration, then the particles would stream out along the field lines. Because of synchrotron losses and the adiabatic invariants in the motion of the particles as they migrate from regions of strong magnetic fields to regions of weaker fields the mean pitch angle would decrease even further.

A large flux of particles with small pitch angles could some about in many of the models suggested for active galactic nuclei (Sturrock

and Barnes, 1972; Morrison, 1969; Lynden-Bell, 1969 or Piddington, 1970) if clouds of relativistic particles are repeatedly ejected from a compact central source; the particles then would stream out along the field lines driving away the ambient interstellar gas and dragging the magnetic field into an open configuration, just as the solar wind determines the structure of the interplanetary magnetic field. In the cavity which is formed in this manner, the relativistic electrons would travel with small pitch angles and emit synchrotron radiation.

Possible source parameters for the small-pitch-angle models of PKS 2134 + 004 and OQ 208 are given in Table 2 and the corresponding spectra are shown by the solid curves in Figure 8. The index s, the characteristic pitch angle $\tilde{\Psi}$, and the energies γ_1 and γ_2 are defined by equation (2.43). The magnetic field has been computed from the requirement that the source must be optically thin to synchrotron self-absorption. A simple thermodynamic argument (Scheuer and Williams, 1968) shows that when $\bar{\gamma}\,\bar{\Psi} \ll 1$ a source of flux density F and angular size θ is optically thin to synchrotron self-absorption if

$$B \leq 0.2 \text{ gauss}[\nu(1+z)/\text{GHz}]^3(\theta/.001")^2[F(\nu)]^{-1} \qquad (3.3)$$

where F is in flux units (1 f.u. = 10^{-26} $\text{Wm}^{-2}\text{Hz}^{-1}$).

TABLE 2 - SMALL-PITCH-ANGLE MODELS

Source	PKS 2134 + 004	OQ 208
B (gauss)	0.1	1.0
s	2.5	3.0
γ_1	3.0×10^4	3.0×10^3
γ_2	$\geq 5 \times 10^5$	$\geq 3 \times 10^4$
$\tilde{\psi}$	10^{-5}	10^{-4}

In Chapter 2 it was shown that for the synchrotron radiation from particles with small pitch angles the degree of circular polarization is often very high while the amount of linear polarization is normally small. For source distributions which are spearable in energy and pitch angle and have low energy cutoffs (Equation 2.43), the degree of circular polarization approaches 100% at lower frequencies (Figures 5 and 7) and the sense of the polarization (right handed or left handed) reverses near the frequency at which the emissivity is a maximum (as mentioned in Chapter 2 the reversal sign is not unique to this model). No observation has yet revealed a very high degree of circular polarization for any extragalactic objects; however, in an actual galactic nucleus the degree of circular polarization could be much smaller if the magnetic field has sectors of opposite polarity similar to those of the interplanetary magnetic field (Wilcox, 1968) or if particles of opposite charge contribute to the emission. The degree of linear polarization is

even more sensitive to the structure of the magnetic field (Equation 2.42) and slight irregularities in the field can reduce the amount of linear polarization considerably. Consequently for small-pitch-angle models of PKS 2134 + 004 and OQ 208, the degree of linear polarization could be small and the circular polarization should reverse its sense near the frequency of the peak ν_m and become stronger at lower frequencies. There are no published polarization measurements for frequencies greater than ν_m for these objects, but the observed degree of circular polarization for the low frequency emission from PKS 2134 + 004 is unusually high (see item (B) below) and does show some decrease with increasing frequency. Additional measurements for both PKS 2134 + 004 and OQ 208 especially over a wide frequency interval, are desirable.

Admittedly these models for PKS 2134 + 004 and OQ 208 are overly complex (considering the number of observed features on which they are based) and unrealistically simple (since the radiation from electrons with either large pitch angles or energies below $\gamma_1 mc^2$ is totally neglected); nevertheless, these models do serve to illustrate some of the possible features of synchrotron sources in which the electrons stream with small pitch angles. In some sources, conventional synchrotron radiation and self-absorption might also be significant so that the characteristics mentioned above would be somewhat obscured; the only evidence for particles with small pitch angles would then be an anomalously high degree of circular polarization.

Cavaliere et al. (1970) suggested that the large infrared radiation from objects such as the quasar 3C 273 and some of the Seyfert galaxies including NGC 1068 is synchrotron emission from electrons with small

pitch angles. These authors assumed that the low frequency infrared emission could fall off rapidly due to the "cyclotron turnover" (O'Dell and Sartori, 1970b), but as shown in Chapter 2 this is not the case. The low frequency falloff in the emission from an optically thin synchrotron source cannot be much steeper than $F \propto \nu$. Even if the peak of the infrared emission from NGC 1068 occurs at 22μ, this falloff is not abrupt enough to be consistent with both the infrared and the millimeter flux densities (see solid curve of Figure 9). The model of Cavaliere et al. could be modified by assuming that some absorption process is responsible for suppressing millimeter emission, but then the main motivation for suggesting that the electrons have small pitch angles no longer exists. Unless some new data becomes available (for instance, measurements of strong infrared circular polarization), there does not appear to be any need to pursue small-pitch-angle models of NGC 1068.

B) Self-Absorption Models

Low frequency cutoffs are commonly attributed to synchrotron self-absorption. As we shall see below this interpretation encounters difficulty for some sources which exhibit high degree of circular polarization.

For a homogeneous spherical source which is synchrotron self-absorbed the flux density in flux units is (Terrell, 1967)

$$F(\nu) = 0.48\left(\frac{\nu}{\mathrm{GHz}}\right)^{5/2} \frac{(\theta/.001'')^2 (B/10^{-2}\mathrm{gauss})^{-1/2}}{(1 + .31\alpha + .039\alpha^2)(1+z)^{1/2}} \qquad (3.4)$$

where z is the redshift, B is the characteristic strength of the

magnetic field, θ is the average angular diameter and α is the spectral index at high frequencies where the source is transparent. The self-absorbed spectra for PKS 2134 + 004, OQ 208 and NGC 1068 are illustrated by the dashed curves in Figures 8 and 9.

It is clear that the spectral shapes for the radio sources do not agree with this simple model for self-absorption; however, if PKS 2134 +004 and OQ 208 are non-uniform or comprise several components, it is entirely possible that relatively slow falloffs could result from synchrotron self-absorption (see Hirasawa and Tabara, 1970, for example). Additional high angular resolution observations of these objects would be useful to determine whether the low frequency emission is due to the presence of more than one component.

If one assumes that the turnover in an emission spectrum is due to synchrotron self-absorption, then equation (3.4) yields an expression for the magnetic field strength in the source in terms of observable quantities. Once B is known, other source parameters can be computed, for example, the degree of circular polarization of the synchrotron radiation, $P_c \sim \left[\frac{\nu_B}{\nu(1+z)}\right]^{1/2}$ (Legg and Westfold, 1968; note that the emitted frequency $(1+z)\nu$ should be used in their equations), and the inverse Compton x-ray flux density which results from the scattering of the radio frequency photons by the relativistic electrons (Blumenthal and Gould, 1970). In Table 3 we have listed possible sets of source parameters for synchrotron self-absorption models of PKS 2134 + 004, OQ 208 and NGC 1068. A Hubble parameter of 75 km/(sec Mpc) and a relativistic cosmological model with zero cosmological constant and with $q_o = 1$ have been used.

TABLE 3 - SELF-ABSORPTION MODELS

Source	PKS 2134 + 004 [b]		OQ 208	NGC 1068
θ^2 (seconds of arc)^2	5×10^{-7}	4×10^{-6}	3×10^{-6}	8×10^{-10}
d (cm)	9.5×10^{18}	2.6×10^{19}	7.1×10^{18}	7.0×10^{15}
B (gauss)	2.8×10^{-3}	1.5×10^{-1}	3.2×10^{-1}	2.8×10^{2}
$P_c(\nu_m)$ %	.06	.43	1.3	1.1
ν_{IC} (Hz) [a]	7.8×10^{16}	1.4×10^{15}	9.6×10^{13}	1.5×10^{17}
F_{IC}(erg sec^{-1}Hz^{-1}cm^{-2}) [a]	1.2×10^{-26}	3.1×10^{-29}	2.2×10^{-31}	8.3×10^{-27}

The quantities in column 1 are: θ, the angular diameter; d, the linear diameter; B, the characteristic magnetic field strength; $P_c(\nu_m)$, the degree of circular polarization at the peak of the synchrotron spectrum; ν_{IC}, the frequency at which the inverse Compton emission is a maximum; and F_{IC} the inverse Compton flux density at ν_{IC}.

(a) The tabulated value of ν_{IC} and F_{IC} are upper and lower bounds, respectively, which were obtained by assuming that the distributions of relativistic electrons cutoff below $\gamma = 10^{-3}\nu_m^{1/2}B$.

(b) A maximum flux density of 7.5 f.u. was used since the interferometric work of Cohen et al. (1971) indicated that only about 56% of the radio flux may come from a single compact component.

With the observed angular size for PKS 2134 + 004, the self-absorption model predicts that the degree of circular polarization will be considerably lower than the observed value and that the x-ray flux due to the inverse Compton process would be very large (about six times greater than that of NGC 1275 at 10^{18} Hz; Gursky et al., 1971). The discrepancy between the observed and predicted amounts of circular polarization is strong evidence against the self-absorption model; however this result is very dependent on the angular structure of the source. If the source was elongated so that it has angular size of about 0".006 in some direction then the mean value of θ^2 would be 4×10^{-6} and it would be possible to reconcile the self-absorption model with the observed degree of circular polarization as shown by the second set of numbers in Table 3 for this source. With this larger size the model is consistent with the observed circular polarization and predicts an inconsequential x-ray flux.

The self-absorption interpretation for OQ 208 requires a large magnetic field strength and predicts that the radiation should exhibit a high degree of circular polarization (Table 3). Measurements of polarization and angular structure of the radio emission could be of considerable interest and would permit the self-absorption model to be evaluated.

For the infrared source in NGC 1068, only upper limits are available for the angular size, the 50μ flux, and the x-ray flux. To specify the parameters for the synchrotron-self-absorption models we have used criteria similar to those of Bergeron and Salpeter (1971): (1) We fit a power law to the infrared data and assumed that the peak occurs at 50μ

(as shown by the dashed curve in Figure 9), and we assumed that the x-ray flux at 7.5×10^{17} Hz was equal to 10^{-5} f.u., one half of the observed upper limit. The source parameters shown in Table 3 were then computed for a spectral index of $\alpha = 2.5$. There are no observations in conflict with this model: the small size is consistent with the observed variations and the polarization measurements have only been made at higher frequencies and are not necessarily related to the infrared emission. A possible test of the self-absorption model would be to measure the infrared polarization to see if it exhibits the large degree of linear polarization characteristic of synchrotron sources and the small degree of circular polarization which is listed in Table 3.

C) Thermal-Absorption Models

The bright emission lines from quasars and Seyfert galaxies are evidence for the presence of large amounts of thermal gas which could account for the low frequency turnovers in the spectra of some sources (Allen, 1968; Weymann, 1970). For example, the model for the line emitting region of 3C 48 proposed by Bahcall and Kozlovsky (1969) would be opaque to radio waves of frequency less than about 10 GHz. Similarly, Weymann (1970) found that the strong, broad wings in the hydrogen Balmer lines from the Seyfert galaxy NGC 4151 may indicate the presence of very dense gas which would absorb most of the far infrared radiation impinging on it.

To study the effects of thermal absorption in synchrotron sources we have used the following simple model: A synchrotron source of radius r_1 is imbedded in a cloud of thermal gas of radius r_2 ($r_2 \geq r_1$). The intensive properties of the gas (the electron temperature, T_e; the

mean electron density, n_e; and the filling factor, ϵ) and of the synchrotron source (the particle distribution and the magnetic field strength, B) are assumed to be uniform throughout the respective spheres. For this model the observed flux density is approximately given by

$$F(\nu) = f(\nu) \frac{e^{-\tau_o}}{\tau_i} \left[1 - e^{-\tau_i}\right], \qquad (3.5)$$

where we have ignored the effects of the non-planar geometry and the emission from the thermal gas. In equation (3.5) $f(\nu)$ is the spectrum which would be observed if there were no absorption: we assume $f \propto \nu^{-\alpha}$ for frequencies greater than $\nu_1 = 1.2 \times 10^6 \gamma_1^2 B$, where $\gamma_1 mc^2$ is the energy below which the distribution of the relativistic electrons cuts off. The optical depth τ_i takes into account the absorption by the material within radius r_1 and includes both the effects of the thermal absorption and the synchrotron self-absorption. The term $e^{-\tau_o}$ represents the effect of absorption by the shell of thermal gas (thickness $r_2 - r_1$) which surrounds the synchrotron source. When the electron scattering optical depth, τ_{es}, is small compared to the free-free optical depth, τ_{ff}*, the thermal absorption optical depth is given by τ_{ff}. When τ_{es} exceeds τ_{ff} the diffusion approximation for the optical depth can be used; $\tau_{diff} \approx \sqrt{3\, \tau_{es} \tau_{ff}}$ (Tucker, 1967).

For the radio sources PKS 2134 + 004 and OQ 208 the logarithmic slope of spectrum changes by about 2 near the peak of the spectra, ν_m, and the low frequency falloff continues as a power law down to at least

*In c.g.s units $\tau_{es} = 6.65 \times 10^{-25} \int n_e dr$ and $\tau_{ff} = \zeta \nu^{-2} \int n_e^2 T^{-3/2} dr$; $\zeta \approx .16$ for the parameters of the radio sources and $\zeta \approx .10$ for those of NGC 1068; (Karzas and Latter, 1961).

$0.1\ \nu_m$. In terms of the thermal-absorption model this implies that $\nu_1 \leq 0.1\ \nu_m$ and $\tau_{es} \ll 1$, and that at $\nu = 0.1\ \nu_m$ the self-absorption optical depth is much less than τ_{ff} and $\tau_o \ll 1$. Source parameters for PKS 2134 + 004 and OQ 208 which satisfy these conditions are listed in Table 4 and the corresponding spectra are shown by the dotted curves in Figure 8. Following Bahcall and Kozlovsky (1969), we have used $T_e = 1.7 \times 10^4\ ^oK$ and $\epsilon = 10^{-3}$. The radius r_1 is determined from the observed angular diameter, and we have set $r_2 = r_1$ so that $\tau_o = 0$.

The thermal-absorption model of PKS 2134 + 004 encounters difficulties which are similar to, but much more severe than, those of the self-absorption model. The condition that the synchrotron self-absorption is insignificant requires a weak magnetic field so that the degree of circular polarization is much less than the observed value and the inverse Compton x- and γ-radiation is totally unreasonable (over 10^{56} erg/sec $\sim 10^{24}\ L_\odot$). The thermal absorption interpretation for the spectrum of OQ 208 fares somewhat better. The source parameters are plausible, and the shape of the theoretical spectrum agrees well with the observation. An attractive feature of this model is that its predictions permit it to be tested. The radio emission should have a small, perhaps marginally detectable, degree of circular polarization whereas the degree of linear polarization, P_ℓ, should be largely eradicated by the Faraday depolarization. [For a uniform source $P_\ell \leq$ (Faraday rotation in radians)$^{-1}$ = $(RM \times c^2/\nu_m^{\,2})^{-1} \approx 0.1\%$. But P_ℓ could be somewhat larger for a non-uniform source.] Furthermore, the weak x-radiation from the inverse Compton process might also be detectable.

TABLE 4 - THERMAL-ABSORPTION MODELS

Source	PKS 2134 + 004	OQ 208	NGC 1068
r_1 (cm)	4.7×10^{18}	3.5×10^{18}	8.0×10^{15}
r_2 (cm)	4.7×10^{18}	3.5×10^{18}	8.8×10^{15}
n_{ec} (cm^{-3})	1.6×10^{5}	3.7×10^{5}	3.6×10^{9}
T_e (^oK)	1.7×10^{4}	1.7×10^{4}	8.0×10^{4}
ϵ	10^{-3}	10^{-3}	10^{-1}
B (gauss)	2.0×10^{-7}	7.5×10^{-4}	1.3×10^{2}
γ_1	5.3×10^{4}	1.2×10^{3}	1.0×10^{2}
$P_c(\nu_m)$ (%)	.0049	.045	.78
RM (radians/cm^2)	4.4×10^{-4}	25	3.8×10^{8}
ν_{IC} (Hz)	9.2×10^{19}	1.1×10^{16}	1.0×10^{17}
F_{IC}(erg $sec^{-1}Hz^{-1}cm^{-2}$)	6.9×10^{-22}	1.6×10^{-27}	1.4×10^{-26}

The quantities in the first column are as follows: ϵ is the filling factor, that is the fraction of source volume occupied by the thermal gas; n_{ec} is the electron density in clouds or filaments (note $\int_o^R n_e^m dr \approx n_{ec}^m \epsilon R$, for $m > 0$); RM is the Faraday rotation measure (RM = $2.62 \times 10^{-17} \int_o^R n_e B \cos\theta \, dr$; we assume that $\cos\theta \approx 1/2$); and the other parameters are defined in Table 3 and the text.

As was mentioned above the presence of dense gas in the nuclei of Seyfert galaxies was inferred from the existence of the wide wings on the hydrogen Balmer lines; however, it may be that these regions of dense gas occur in the nuclei of all the Seyfert galaxies, even in those galaxies, such as NGC 1068, which do not emit Balmer lines with broad wings. Weymann (1970) suggested that the powerful infrared source of NGC 1068 might be located within one of these dense clouds so that the far infrared cutoff would be due to thermal absorption by this gas. We have examined this suggestion in terms of the thermal-absorption model to see whether a consistent source description could be obtained.

The features which must be incorporated in a satisfactory thermal-absorption model for NGC 1068 are as follows: (1) The onset of appreciable thermal absorption occurs below ν_m ($= 6 \times 10^{12}$Hz) yet (2) the cutoff is steep enough to be consistent with the millimeter observations. (3) The thermal gas re-emits all the energy it absorbs; while (4) the free-free emission from the gas is less than the observed x-radiation; and (5) the Hβ luminosity of the gas does not exceed the observed value for the entire nucleus ($F_{H\beta} = 1.26 \times 10^{-12}$erg sec^{-1}cm^{-2}; Osterbrock and Parker, 1965). (6) The synchrotron self-absorption is small compared to thermal absorption, and (7) the inverse Compton emission is consistent with the x-ray observations. The first and third conditions yield n_e and r_2 as functions of T_e, γ_1, and ϵ. Conditions (3), (4) and (5) set the bounds $6 \times 10^4\ ^oK \leq T_e \leq 5 \times 10^6\ ^oK$ on the temperature of the gas (the cooling rate of the gas was taken from Cox and Tucker, 1969; and the Hβ luminosity was calculated from Table IV of Pengelly, 1964). If we impose the additional constraint that the gas be stable against

thermal instabilities (Field, 1965) then T_e must be less than $\sim 10^5$ °K. Condition (2) requires that r_1 be somewhat smaller than r_2 (so that the low frequency cutoffs in equation (3.5) are exponential for $\nu \leq 3 \times 10^{11}$); whereas conditions (6) and (7) give an upper and lower limit, respectively, on the magnetic field strength in terms of r_1. These conditions do not yield a unique description of the thermal-absorption model of NGC 1068, but they constrain the range of acceptable source parameters. One set of parameters is given in Table 4 and the corresponding spectrum is shown by the dotted curve in Figure 7.

A striking feature of this model is that the size and field strength of the synchrotron source are very similar to those of the self-absorption model. If models are judged on how few assumptions are needed to explain a given number of observations, then the thermal-absorption model for NGC 1068 comes out badly; it requires essentially the same type of synchrotron source as the self-absorption model (one with a very small size and intense magnetic field), and in addition it requires a compact cloud of very high density gas. A more important test of any model is its predictive value. Both the self-absorption model and the thermal-absorption model predict a small amount of circular polarization in the infrared; however, in the thermal-absorption model Faraday depolarization will eliminate the possibility of more than a few per cent linear polarization below 3×10^{13} Hz.

IV. Discussion

Using the results of Chapter 2 for synchrotron emission from particles with small pitch angles we have placed some constraints on possible models for the radiation from optical pulsars and certain compact extragalactic objects.

The nearly cusp-like variations of the optical intensity from the Crab Nebula pulsar, NP 0532, and the lack of any observable circular polarization precludes the possibility that this radiation is due to incoherent electron synchrotron emission from the corotating portion of the pulsar magnetosphere. The results which we have derived for electron synchrotron emission can be modified for models in which the synchrotron emission is produced by protons or a mixture of positrons and electrons. The restrictions would not be as severe for these cases and would only represent bounds on the acceptable range of parameters.

We have considered three extragalactic compact sources which have low frequency cutoffs in their spectra. Two of the sources, the quasar PKS 2134 + 004 and the Seyfert galaxy OQ 208, have low frequency flux densities nearly proportional to frequency, as would be expected from electron distributions with small pitch angles (Figures 5 and 7). The third source, NGC 1068, is strong infrared emitter which cuts off steeply at far-infrared. We have investigated whether the low frequency spectra of these sources could be due to emission by particles with small pitch angles, or absorption by thermal plasma or synchrotron self-absorption.

The available data on the spectrum, size and polarization of PKS 2134 + 004 supports the small-pitch-angle model, but cannot be reconciled with the self-absorption or the thermal-absorption models

unless the source is greatly elongated. Additional measurements of angular structures and searches for x-ray flux would allow a more definite comparison of these models. The observed radio spectrum of OQ 208 can be reproduced by either the small-pitch-angle model and the thermal-absorption model, while the self-absorption model would require that this source has a complex angular structure. Measurements of the radio polarization of OQ 208 would be useful for further judging these models, and searches for a soft x-ray flux might also yield positive results. Some circular polarization should be detectable if either the small-pitch-angle or self-absorption interpretation is correct, whereas observations of a large degree of linear polarization would argue against the small-pitch-angle and thermal-absorption models. If the thermal-absorption model is valid, there would also be an appreciable flux of soft x-rays from OQ 208.

The steep cutoff in the far-infrared emission of NGC 1068 does not agree with the small-pitch-angle model, but it can be explained by either the self-absorption or the thermal-absorption model; the self-absorption model requires somewhat simpler assumptions. Measurements of the infrared polarization would be required to evaluate these models. For the self-absorption model there might be the high degree of linear polarization which is characteristic of the synchrotron process, but for the thermal-absorption model the linear polarization would be weak and very frequency dependent due to the large amount of Faraday depolarization.

APPENDIX

Coefficients for Equations 2.49 and 2.50

$$c_1 = \frac{1}{2(s-1)}$$

$$c_2 = \frac{2}{3^{1/3}(3s-1)}$$

$$c_3 = \frac{3^{s/2}\Gamma\left(\frac{3s-1}{12}\right)\Gamma\left(\frac{3s+19}{12}\right)\Gamma\left(\frac{s+1}{4}\right)}{8\pi}$$

$$c_4 = \frac{3s-1}{3^{1/3}(3s+4)}$$

$$c_5 = \frac{s\,\Gamma\left(\frac{3s+8}{12}\right)\Gamma\left(\frac{3s+4}{12}\right)\Gamma\left(\frac{s}{4}\right)}{2\,3\,\Gamma\left(\frac{3s-1}{12}\right)\Gamma\left(\frac{3s+19}{12}\right)\Gamma\left(\frac{s+1}{4}\right)}$$

TABLE 5

s	c_1	c_2	c_3	c_4	c_5
1.0	--	.69	.64	.20	.18
1.5	1.00	.40	.39	.29	.30
2.0	.50	.28	.32	.35	.40
2.5	.33	.21	.31	.39	.48
3.0	.25	.17	.33	.43	.56
3.5	.20	.15	.39	.45	.63
4.0	.16	.13	.48	.48	.69
4.5	.14	.11	.63	.50	.74
5.0	.13	.10	.88	.51	.80

REFERENCES

Alfvén, H. and Herlofson, N., (1950), Phys. Rev. 78, 616.

Allen, C.W., (1963), Astrophysical Quantities (Second Edition, London: Athene Press).

Allen, R.J., (1968), Ap. J. 153, 389.

Andrew, B.H., Medd, W.J., Harvey, G.A. and Locke, J.L., (1972), Nature 236, 445.

Baade, W., (1956), Ap. J. 123, 550.

Bahcall, J.N. and Kozlovsky, B., (1969), Ap. J. 158, 529.

Bekefi, G., (1966), Radiation Processes in Plasmas (New York: John Wiley and Sons).

Berge, G.L. and Seielstad, G.A., (1972), preprint.

Bergeron, J. and Salpeter, E.E., (1971), Astrophys. Letters 9, 121.

Blake, G.M., (1970), Astrophys. Letters 6, 201.

Blake, G.M., Argue, A.N. and Kenworthy, C.M., (1970), Astrophys. Letters 6, 167.

Blumenthal, G.R. and Gould, R.J., (1970), Rev. Mod. Phys. 42, 237.

Broderick, J.J., Vitkevich, V.V., Jauncey, D.L., Efanov, V.A., Kellermann, K.I., Clark, B.G., Kogan, L.R., Kostenko, V.I., Cohen, M.H., Matveenko, L.I., Moiseev, I.G., Payne, J. and Hansson, B., (1971), Sov. Astron. AJ 14, 627 (translated from Astronomicheskii Zhurnal 47, 784, 1970).

Burbidge, E.M., Burbidge, G.R. and Prendergast, K.H., (1959), Ap. J. 130, 26.

Cavaliere, A., Morrison, P. and Pacini, F., (1970), Ap. J. Letters 162, L133.

Cocke, W.J., Muncaster, G.W. and Gehrels, T., (1971), Ap. J. Letters 169, L119.

Cocke, W.J., Disney, M.J., Muncaster, G.W. and Gehrels, T., (1970), Nature 227, 1327.

Cohen, M.H., Cannon, W., Purcell, G.H., Shaffer, D.B., Broderick, J.J., Kellermann, K.I. and Jauncey, D.L., (1971), Ap. J. 170, 207.

Cox, D.P. and Tucker, W.H., (1969), Ap. J. 157, 1157.

Elder, F.R., Langmuir, R.V. and Pollock, H.C., (1948), Phys. Rev. 74, 52.

Epstein, R.I. and Feldman, P.A., (1967), Ap. J. Letters 150, L109.

Felten, J.E. and Rees, M.J., (1972), Astron. and Astrophys. 17, 226.

Field, G.B., (1965), Ap. J. 142, 531.

Ginzburg, V.L. and Syrovatskii, S.I., (1965), Ann. Rev. Astron. and Astrophys. 3, 297.

Ginzburg, V.L. and Syrovatskii, S.I., (1969), Ann. Rev. Astron. and Astrophys. 7, 375.

Gursky, H., Kellogg, E.M., Leong, C., Tananbaum, H. and Giacconi, R., (1971), Ap. J. Letters 165, L43.

Hirasawa, T. and Tabara, H., (1970), Astrophys. Letters 7, 121.

Hornby, J.M. and Williams, P.J.S., (1966), M.N.R.A.S. 131, 237.

Karzas, W.J. and Latter, R., (1961), Ap. J. Supp. 6, 167.

Jauncey, D.L., Neill, A.E. and Condon, J.J., (1970), Ap. J. Letters 162, L31.

Kellermann, K.I. and Pauliny-Toth, I.I.K., (1971), Astrophys. Letters 8, 153.

Kellermann, K.I., Clark, B.G., Jauncey, D.L., Cohen, M.H., Shaffer, D.B. and Moffet, A.T., (1970), Ap. J. 161, 803.

Kemp, J.C., Wolstencroft, R.D. and Swedlund, J.B., (1972), Ap. J. Letters 173, L113.

Kleinmann, D.E. and Low, F.J., (1970), Ap. J. Letters 159, L165.

Kraus, J.D. and Andrew, B.H., (1970), Ap. J. Letters 159, L41.

Kraus, J.D. and Scheer, D.J., (1967), Ap. J. Letters 149, L111.

Kruszewski, A., (1968), Astron. J. 73, 852.

Legg, M.P.C. and Westfold, K.C., (1968), Ap. J. 154, 499.

Lerche, I., (1970), Ap. J. 162, 153.

LeRoux, E., (1961), Ann. Ap. 24, 71.

Low, F.J. and Rieke, G.H., (1971), Nature 233, 256.

Lynden-Bell, D., (1969), Nature 223, 690.

Medd, W.J., Andrew, B.H., Harvey, G.A. and Locke, J.L., (1972), in preparation.

Melrose, D.B., (1971a), Astrophys. Letters 8, 35.

Melrose, D.B., (1971b), Astrophys. Sp. Sci. 12, 172.

Morrison, P., (1969), Ap. J. Letters 157, L73.

Neugebauer, G., Garmire, G., Rieke, G.H. and Low, F.J., (1971), Ap. J. Letters 166, L45.

Noerdlinger, P.D., (1969), Astrophys. Letters 4, 233.

O'Dell, S.L. and Sartori, L., (1970a), Ap. J. Letters 161, L63.

O'Dell, S.L. and Sartori, L., (1970b), Ap. J. Letters 162, L37.

Oort, J.H. and Walraven, J.H., (1956), B.A.N. No. 462.

Osterbrock, D.E. and Parker, R.A.R., (1965), Ap. J. 141, 892.

Pacholczyk, A.G., (1970), Radio Astrophysics (San Francisco, W.H. Freeman).

Pacholczyk, A.G. and Swihart, T.L., (1970), Ap. J. 170, 405.

Papaliolios, C., Carleton, N.P. and Horowitz, P., (1970), Nature 228, 445.

Pauliny-Toth, I.I.K. and Kellermann, K.I., (1968), Ap. J. Letters 152, L169.

Pengelly, R.M., (1964), M.N.R.A.S. 127, 145.

Piddington, J.H., (1970), M.N.R.A.S. 148, 131.

Ramaty, R., (1969), Ap. J. 158, 753.

Razin, V.A., (1958), Astron. Zh. 35, 241 (translated in Soviet Astron. AJ 2, 216, 1958).

Rieke, G.H. and Low, F.J., (1972), Ap. J. Letters 176, L95.

Roberts, J.A., Ribes, J.C., Murray, J.D. and Cocke, D.J., (1972), Nature Phys. Sci. 236, 3.

Scheuer, P.A.G. and Williams, P.J.S., (1968), ARAA 6, 321.

Schwinger, J., (1949), Phys. Rev. 75, 1912.

Shimmins, A.J., Searle, L., Andrew, B.H. and Brandie, G.W., (1968), Astrophys. Letters 1, 167.

Shklovsky, I.S., (1970), Ap. J. Letters 159, L77.

Speiser, T.W., (1965), J. Geophys. Res. 70, 4219.

Sturrock, P.A., (1971), Ap. J. 164, 529.

Sturrock, P.A. and Barnes, C., (1972), Ap. J. 176, 31.

Tademaru, E., (1972), Ap. J. 172, 327.

Terrell, J., (1967), Ap. J. 147, 827.

Tucker, W.H., (1967), Ap. J. Letters 149, L105.

Walker, M.F., (1968), Ap. J. 151, 71.

Westfold, K.C., (1959), Ap. J. 130, 241.

Weymann, R., (1970), Ap. J. Letters 161, L21.

Woltjer, L., (1966), Ap. J. 146, 597.

Zheleznyakov, V.V., (1972), Cosmic Plasma Physics (Proceedings of the Conference on Cosmic Plasma Physics held at the European Space Research Institute, Frascati, Italy, Sept. 22-24, 1971) (London: Plenum Press), p. 249.

UNCLASSIFIED
Security Classification

DOCUMENT CONTROL DATA - R & D

(Security classification of title, body of abstract and indexing annotation must be entered when the overall report is classified)

1. ORIGINATING ACTIVITY *(Corporate author)*
Institute for Plasma Research
Stanford University
Stanford, California 94305

2a. REPORT SECURITY CLASSIFICATION
UNCLASSIFIED

2b. GROUP

3. REPORT TITLE
Some Aspects of Cosmic Synchrotron Sources

4. DESCRIPTIVE NOTES *(Type of report and inclusive dates)*
Scientific Interim

5. AUTHOR(S) *(First name, middle initial, last name)*
Richard I. Epstein

6. REPORT DATE
31 January 1973

7a. TOTAL NO. OF PAGES

7b. NO. OF REFS

8a. CONTRACT OR GRANT NO.
N00014-67-A-0112-0062

b. PROJECT NO.
NR 323-009

c.

d.

9a. ORIGINATOR'S REPORT NUMBER(S)
SUIPR Report No. 435

9b. OTHER REPORT NO(S) *(Any other numbers that may be assigned this report)*

10. DISTRIBUTION STATEMENT
This document has been approved for public release and sale; its distribution is unlimited.

11. SUPPLEMENTARY NOTES
TECH, OTHER

12. SPONSORING MILITARY ACTIVITY
Office of Naval Research
800 North Quincy Street
Arlington, Virginia 22217

13. ABSTRACT

In the earlier treatments of synchrotron theory it was usually assumed that the pitch angles of the radiating particles are of the order of unity and that the emission occurs at high harmonics of the fundamental frequency. In this investigation we have examined synchrotron radiation for some of the cases for which these assumptions are not applicable. We first considered the synchrotron emission from individual particles which have small pitch angles, the general properties of synchrotron sources which mainly contain such particles, and the emissivities and degrees of circular polarization for specific source distributions. We then considered several models for actual synchrotron sources. The limitation of synchrotron source models for optical pulsars and compact extragalactic objects are discussed and it is shown that several existing models for the pulsar NP 0532 are inconsistent with the measured time variations and polarizations of the optical emission. We also consider whether the low frequency falloffs in the extragalactic objects PKS 2134 + 004, OQ 208 and NGC 1068 could be due to emission from particles with small pitch angles or absorption by a thermal plasma or synchrotron self-absorption. Emission by particles with small pitch angles could explain the observations of PKS 2134 + 004 and OQ 208 but is inconsistent with the data for NGC 1068. The absorption interpretations cannot account for the turnover in the spectrum of PKS 2134 + 004. Measurements of polarization, angular structure and x-ray flux which would be helpful in evaluating these models are described.

DD FORM 1 NOV 68 1473

UNCLASSIFIED
Security Classification

UNCLASSIFIED

Security Classification

14. KEY WORDS	LINK A		LINK B		LINK C	
	ROLE	WT	ROLE	WT	ROLE	WT
SYNCHROTRON RADIATION						
PULSAR						
QUASAR						
SEYFERT GALAXY						

UNCLASSIFIED

Security Classification